

This version of the article has been accepted for publication, after peer review (when applicable) but is not the Version of Record and does not reflect post-acceptance improvements, or any corrections.

The Version of Record is available online at: <http://dx.doi.org/10.1038/s43017-022-00309-5>.

Use of this Accepted Version is subject to the publisher's Accepted Manuscript terms of use <https://www.springernature.com/gp/open-research/policies/acceptedmanuscript-terms>.

## Stability of the Antarctic Ice Sheet during the pre-industrial Holocene

Richard S. Jones<sup>1,2†</sup>, Joanne S. Johnson<sup>3</sup>, Yucheng Lin<sup>4</sup>, Andrew N. Mackintosh<sup>1,2</sup>, Juliet P. Sefton<sup>5</sup>, James A. Smith<sup>3</sup>, Elizabeth R. Thomas<sup>3</sup> and Pippa L. Whitehouse<sup>4</sup>

<sup>1</sup> Earth Atmosphere and Environment, Monash University, Clayton, Victoria, Australia

<sup>2</sup> Securing Antarctica's Environmental Future, Monash University, Clayton, Victoria, Australia

<sup>3</sup> British Antarctic Survey, Cambridge, U.K.

<sup>4</sup> Department of Geography, Durham University, Durham, U.K.

<sup>5</sup> Earth and Ocean Sciences, Tufts University, Medford, MA, U.S.A.

†email: [richard.s.jones@monash.edu](mailto:richard.s.jones@monash.edu)

### Abstract

The rate and magnitude of the Antarctic Ice Sheet (AIS) contribution to global sea-level rise beyond 2100 CE remains highly uncertain. Past changes of the AIS, however, offer opportunities to understand contemporary and future ice sheet behaviour. In this Review, we outline how the AIS evolved through the pre-Industrial Holocene, 11,700 years ago to 1850 CE. Three main phases of ice sheet behaviour are identified: a period of rapid ice volume loss across all sectors in the Early and Mid Holocene; a retreat inland of the present-day ice sheet margin in some sectors, followed by readvance; and continued ice volume loss in several sectors during the past few millennia, and in some areas up to and into the Industrial era. Global sea levels rose by 2.4–12 m owing to the period of rapid Antarctic ice loss, and possibly fell by 0.35–1.2 m owing to subsequent readvance. Changes in the AIS during the Holocene were likely driven by similar processes to those acting today and predicted for the future, which are associated with oceanic and atmospheric conditions as well as bed topography. Further work is required to better understand these processes, and to quantify Antarctica's contribution to past sea-level change.

## Key Points

- Multiple lines of evidence indicate that the Antarctic Ice Sheet underwent periods of ice volume loss and gain in the Holocene that affected global sea level.
- Rapid ice loss occurred in all ice sheet sectors during the Early-to-Mid Holocene, contributing between 2.4 and 12 m to global mean sea level rise (GMSL).
- Ice sheet readvance occurred in two sectors during the Holocene, which might have caused a fall in global sea levels of 0.35 m, or possibly 1.2 m.
- The ice sheet was mostly at or near its present-day geometry by the Late Holocene, but ice loss and gain continued in some areas into the Industrial era.
- Ice loss was likely caused by oceanic warming, sea-level rise, retrograde bed topography and atmospheric changes, and ice gain was possibly caused by glacial isostatic adjustment and/or climate variability.
- Improved understanding of the Antarctic Ice Sheet in the Holocene will be achieved through targeted data collection, and developments in chronological techniques and numerical modelling.

## Introduction

Polar ice sheets have a pivotal role in the Earth System, regulating the climate and moderating global sea-level change. Satellite observations reveal that the Antarctic Ice Sheet (AIS) — which has a volume equivalent to 57.9 m of potential sea-level rise<sup>1</sup>— has been losing ice volume at an accelerating rate over the past 4 decades<sup>2</sup>. In several sectors, the grounding line — where the ice flowing off the land begins to float — has been retreating, with associated thinning of the ice sheet inland<sup>3,4</sup>. This ice volume loss has been dominated by ice dynamic processes rather than surface melting<sup>5</sup>, and is likely caused by sub-ice melt and thinning of ice shelves owing to an influx of warm ocean water<sup>6,7</sup>. Although concern exists that a tipping point, associated with self-sustaining ice loss, has already been crossed in parts of Antarctica<sup>8,9</sup>, modern observations are not yet sufficient to determine whether the current ice sheet volume loss marks the start of irreversible retreat<sup>10</sup>.

As a result of such ice loss, the AIS contributed to a gradual rise in global mean sea level (GMSL) over the past century<sup>11</sup>. Although the Antarctic contribution has so far been relatively small, the rate and magnitude of sea-level rise from the AIS is set to accelerate this century (Fig. 1). Numerical ice sheet models predict that the AIS will contribute 0.04–0.22 m (medians of endmembers) to GMSL by 2100 CE<sup>12</sup>, and potentially >9 m by 2300 CE<sup>13</sup>. However, these estimates are uncertain, particularly regarding the timing of rapid ice loss due to instabilities, which is a primary cause of the wide spread in projections to 2100 CE<sup>12</sup> (Fig. 1). As a result, current estimates of future sea-level rise lack the necessary precision for effective policy implementation<sup>14</sup>. Therefore, understanding the processes dictating the rate and magnitude of AIS volume loss in this century and beyond is essential.

The Holocene — the current interglacial period, spanning the past 11,700 years — provides crucial context to better understand current and future ice sheet change. GMSL was relatively stable in the Late Holocene (Fig. 1), prior to the start of the Industrial era (1850 CE), providing a baseline to assess historical sea-level change over the past 150 years<sup>15</sup>. In the Early to Mid Holocene, rates of GMSL rise were similar to those predicted by 2100 CE<sup>12,16</sup>, providing a possible analogue for the processes and rates of future accelerated ice sheet volume loss (Fig. 1), taking into account the different specific boundary conditions and climate forcing for future AIS change. Despite the potential insights into current and future changes in GMSL offered by the Holocene, Antarctica's contribution to Holocene sea-level change and the causes of centennial-scale AIS change are not yet well understood.

In this Review, we examine how the AIS changed during the Holocene. We focus primarily on variations in the grounded portion of the ice sheet, as this directly influences global sea level<sup>17,18</sup>. We first outline the broad spatial and temporal patterns of AIS change during this period, and then assess evidence for three key postulated phases of ice sheet change: early rapid ice volume loss; inland retreat and readvance; and final pre-Industrial ice volume change. We then discuss Antarctica's potential contribution to global sea-level change in the Holocene. We conclude by summarising current knowledge of the characteristics and processes of AIS change, and the scientific advances required to better understand ice volume variability and more reliably predict centennial-scale contributions to sea-level rise.

## Context to Holocene AIS history

Based on compilations of Antarctic glacial geological evidence, AIS volume last peaked during the Last Glacial Maximum, approximately 20,000–27,000 years ago<sup>19</sup>. Ice volume substantially decreased over the subsequent millennia, responding to a warming climate, sea-level rise and Earth System feedbacks<sup>19–22</sup>. Since the onset of the Holocene, GMSL has risen by ~62 m and ice loss from the AIS has likely made a substantial contribution to this increase<sup>16,23</sup>. Determining the contribution of the AIS to global sea-level change during the Holocene, including the spatial and temporal pattern of that change, requires knowledge of Antarctica's ice sheet history.

Knowledge of past changes in the volume of grounded ice is based on three main types of evidence: ice thickness change; grounding line migration; and the response to ice load change (Box 1). Although this evidence provides the most direct indication of ice sheet volume change, past changes in the ice sheet can also be inferred from a variety of proxy records, including: ice volume variability from deep-sea oxygen isotope values<sup>24</sup>; the flux of icebergs (and implied rate of ice shelf calving) from iceberg-rafted debris found in marine sediment<sup>20</sup>; glacial discharge (melting of grounded or floating glacial ice) from the isotopic signature of marine microfossils<sup>25</sup>; ice shelf retreat and glacier melt from the isotopic signature of marine and lacustrine sediments<sup>26,27</sup>; ice flow changes from englacial radar and seismic measurements<sup>28</sup>; a presence or absence of grounded ice from the analysis of subglacial sediments<sup>29</sup>; and ice margin retreat from terrestrial glacial and lacustrine deposits<sup>30</sup>. Such empirical data can be used to guide or evaluate numerical ice sheet models that simulate the deglacial evolution of the ice sheet<sup>21,22,29,31–34</sup>, providing insight into key processes through the Holocene.

The thickness of the AIS varied throughout the Holocene, but these changes were not consistent in magnitude or timing across Antarctica (Fig. 2). Cosmogenic exposure age data indicate a greater amount of ice loss occurred in the Early and Mid Holocene than in the Late Holocene<sup>35–38</sup> (Fig. 2a). A broad period of relatively rapid ice sheet thinning is recorded in all sectors between ~11,000 and 5,000 years ago, and the magnitude and timing of thinning varied between sectors throughout the Holocene.

Ice core evidence indicates that the snow accumulation rate at some locations at the onset of the Holocene was greater than during the pre-Industrial (1700–1850 CE), implying probable thickening in the ice sheet interior, while other locations experienced an accumulation rate lower than pre-Industrial<sup>39</sup> (Fig. 2b). This regional variability, with opposing accumulation trends in neighbouring sectors, continued through the Holocene and into the twentieth century<sup>40</sup>.

Evidence of past grounding line migration indicates that retreat to the inner parts of the continental shelf occurred prior to or at the onset of the Holocene<sup>19</sup>, and that final retreat mostly occurred before ~8,000 years ago<sup>41–43</sup> (Fig. 3). However, as with ice sheet thinning, the exact timing and rate of retreat varied across Antarctica. Emerging evidence also suggests that the grounding line in some sectors retreated inland of its present position during the Holocene, followed by a readvance<sup>29,44,45</sup> (Fig. 3).

Variation in the thickness and extent of grounded ice is also reflected in relative sea level records around Antarctica, which represent the solid-Earth response to ice load change. Although these records do not extend back to the onset of the Holocene at most locations and require knowledge of local Earth rheology to absolutely quantify local ice mass change<sup>46</sup>, they imply that Antarctica has lost ice mass since at least the Mid Holocene, with possible temporary mass gains in some regions<sup>47,48</sup> (Fig. 3).

The Holocene history of the AIS can be divided into three phases: a period of relatively rapid ice volume loss in the early part of the Holocene; retreat inland of the present-day grounding line followed by readvance; and continued ice loss into the later part of the Holocene prior to the Industrial era and modern observations. These phases occurred in broad chronological order, but do not correspond precisely with the formal sub-divisions of the Early, Mid and Late Holocene (Fig. 1) and might have overlapped.

## **Early rapid ice loss**

The largest Holocene change in AIS volume likely occurred during the Early and Mid Holocene. In particular, ice sheet thinning was rapid over this time<sup>49</sup>, potentially providing insight into the centennial-scale response and drivers of contemporary accelerated ice loss<sup>5</sup>.

### ***Ice thickness change near the margin***

Cosmogenic exposure data collected from nunataks near the ice sheet margin (Box 1, Supplementary Information) record a pattern of rapid, yet asynchronous, AIS thinning across sectors. In the Amundsen Sea sector, ice sheet thinning started by ~10,000–12,500 years ago<sup>50,51</sup>, with phases of rapid thinning of hundreds of metres (150–560 m) subsequently occurring in eastern and central regions between ~9,000 and 6,000 years ago<sup>35,52</sup>. In the Ross Sea sector, gradual thinning was underway by ~17,000 years ago<sup>38,53–55</sup>, and accelerated in the Holocene. Rapid lowering of the ice surface (by 140–280 m) is recorded at several outlet glaciers along the Transantarctic Mountains, occurring as either a series of accelerated episodes of thinning (at 9,300, 8,400 and 6,300 years ago<sup>38</sup>) or as an apparent continuous period of thinning (~7,500 to 5,000 years ago<sup>54,36,56</sup>).

In the East Antarctic sector, ice surface lowering is recorded from ~13,000–18,000 years ago, with hundreds of metres of thinning recorded at some sites prior to the Holocene<sup>57,58</sup>. Subsequently, rapid thinning in the Lambert Glacier-Amery Ice Shelf system and eastern Dronning Maud Land is recorded from ~11,000 to 9,000 years ago (300 m)<sup>57</sup> and ~10,000 to 5,000 years ago (350 m)<sup>37,59</sup>, respectively. In the Weddell Sea sector, thinning was underway by ~10,000–14,000 years ago<sup>60,61</sup>. The ice surface progressively lowered at relatively moderate rates until 2,500–5,000 years ago at Foundation Ice Stream (central), but was faster at Institute Ice Stream (west), where ~400 m of lowering occurred between 6,500 and 3,500 years ago<sup>61–63</sup>. In the Antarctic Peninsula, ice surface lowering had begun by ~14,000 years ago<sup>64–66</sup>. Data then imply phases of relatively rapid thinning (250–500 m) from 9,400 to 4,500 years ago in the northeast of the sector<sup>67,68</sup>, and from 12,400 to 9,600 and 7,500 to 6,000 years ago on the western and eastern sides of the Peninsula, respectively<sup>65,69,70</sup>.

When cosmogenic data are considered collectively, ice sheet thinning occurred predominantly between ~11,000 and 5,000 years ago (Fig. 2a). In the Early Holocene, rapid thinning was dominant in East Antarctica, the Weddell Sea sector and parts of the Antarctic Peninsula. Most sectors underwent hundreds of metres of thinning in the Mid Holocene, and the largest amount of thinning in every sector occurred between ~8,000 and 6,000 years ago. Time-averaged rates of ice sheet thinning can be estimated from these data, which indicate that many sectors underwent thinning at a rate similar to, or faster than, that observed at today's most rapidly changing outlet glaciers<sup>49</sup>.

### ***Ice thickness change in the interior***

Ice cores from the interior of the AIS tell a more complex story of Early and Mid Holocene ice thickness change (Box 1, Supplementary Information). Snow accumulation rates in East Antarctica (Dome Fuji, Dome C and Dronning Maud Land) remained fairly constant through the Holocene, with variability of less than  $\pm 10$  m per 500 years<sup>39,71</sup> (Fig. 2b). Despite only minor changes in the accumulation rate, a gradual increase in the surface elevation is apparent from inverse flow modelling, indicating a thickening of ~75–80 m at two of these sites (Dome Fuji and Dome C) since the onset of the Holocene<sup>72</sup>. Near the East Antarctic coast (Law Dome, Fig. 3), an ice core record shows increased accumulation during the Early-to-Mid Holocene, possibly implying some thickening, but any changes were complete by ~8,500 years ago<sup>73,74</sup>. Variations in the accumulation rate recorded in the South Pole ice core record<sup>39,75</sup> can be explained by an acceleration of ice flow since the Early Holocene, but this acceleration could have resulted from interior thickening and/or downstream thinning<sup>76</sup>. Relatively low accumulation is recorded at WAIS Divide (Amundsen and Ross Sea sectors) in the Early Holocene (focused at ~11,000–9,000 years ago), which then increased through the Mid Holocene<sup>77</sup>. This trend in accumulation likely corresponds to initial thinning, followed by a thickening after ~7,000 years ago (Fig. 2b)<sup>78</sup>. In the Ross Sea sector, two sites closer to the coast (Siple Dome and Talos Dome) record high accumulation rates at the onset of the Holocene, indicating some thickening, which then reduced after ~10,500 years ago and into the Mid Holocene<sup>39,79</sup>.

Thus, ice thickening likely occurred across much, but not all, of the ice sheet interior in the Early and Mid Holocene. The rate and magnitude of this thickening is unlikely to have counteracted the ice loss nearer the margin recorded by the cosmogenic exposure data, although the absolute contribution to ice volume change is difficult to estimate from existing evidence. However, the interior of the Amundsen and Ross Sea sectors experienced some thinning at this time, which broadly corresponds to the timing of rapid ice sheet thinning recorded near the ice sheet margin (Fig. 2).

### ***Grounding line retreat and mass loss***

A phase of rapid ice sheet thinning near the margin should be reflected downstream in records of grounding line migration and in responses to ice unloading (Box 1, Supplementary Information). Retreat of the grounding line from the outer continental shelf around Antarctica was underway before the Holocene<sup>19</sup>, and available evidence indicates that retreat across the mid- and inner-shelf was largely complete by 8,000 years ago (Fig. 3). However, subtle differences in the timing have been recorded between sectors. In the Amundsen Sea,

accelerated grounding line retreat occurred near the onset of the Holocene, reaching the inner-shelf as early as 11,700 years ago<sup>42,80</sup>. In the Ross Sea, the grounding line retreated from the outer-shelf in the east 11,500 years ago<sup>81</sup>, had reached the mid-shelf by 8,600 years ago<sup>82</sup>, and had retreated 850 km to its modern position on the inner-shelf by ~4,800–7,500 years ago<sup>45,83</sup>. Retreat was possibly delayed in the western Ross Sea, with a period of ice unloading recorded around 7,800-8,200 years ago (Fig. 3)<sup>47,84</sup>.

In East Antarctica, grounding line retreat occurred offshore of Mac.Robertson Land at the onset of the Holocene (11,700 years ago)<sup>43</sup>. Around this time, ice loss also occurred in Prydz Bay, as grounding line retreat to sites beneath the present Amery Ice Shelf was complete by 11,000 years ago and unloading due to ice mass loss became dominant from 9,400 to 7,100 years ago<sup>48,85–88</sup>. Ice loss also occurred in Wilkes Land, where ice unloading and retreat is recorded from 8,500 years ago<sup>89,90</sup>, and in Dronning Maud Land, where final unloading is recorded from ~7,000 years ago<sup>91</sup> (Fig. 3). In the Weddell Sea, grounding line retreat from the outer-shelf occurred between 12,800 and 10,500 years ago, reaching the mid-shelf by 8,500-8,700 years ago in the east, and possibly the inner-shelf by ~5,000 years ago in the west of the sector<sup>92–96</sup>. In the Antarctic Peninsula, the grounding line had reached the mid-shelf in most places prior to the Holocene<sup>97</sup>. Retreat to the inner-shelf occurred by ~9,700 years ago on both sides of the Peninsula<sup>98,99</sup>, which is consistent with the timing of ice unloading in this sector<sup>100,101</sup> (Fig. 3). Evidence of iceberg flux and glacial discharge in the vicinity of the Weddell Sea and Antarctic Peninsula also indicate that episodes of ice loss occurred at this time, peaking between ~11,500 and 9,000 years ago<sup>20,25</sup>.

Around Antarctica, grounding line retreat to the inner continental shelf was typically closely followed by a period of rapid thinning, which was also reflected in records of ice unloading in some locations<sup>35–37,43</sup>. In every sector, multiple types of evidence are consistent with a phase of rapid ice volume loss in the Early-to-Mid Holocene, with the exact timing and magnitude varying around Antarctica.

### ***Model simulations of rapid ice loss***

Ice sheet modelling provides a means to estimate total AIS volume change and to reveal spatial patterns in AIS change by simulating variations in the ice sheet geometry that are recorded by empirical data. When assessing the ice mass change from multiple models with differing climate forcings and model physics<sup>21,22,29,31–34,102,103</sup>, most volume loss in Antarctica is simulated in the Early Holocene, peaking before 11,500 years ago, and at 11,000 to 10,500 and 10,000 to 9,500 years ago (Fig. 4a). The Ross Sea and Weddell Sea sectors are the dominant contributors during peak periods of ice loss, with the Weddell Sea contribution proportionally increasing after 10,500 years ago, and the Ross Sea almost entirely deglaciated by the Mid Holocene. However, considerable differences exist in the location and magnitude of simulated ice thickness change between models in the Early Holocene, particularly for the Weddell Sea sector in both the Early and Mid Holocene (Fig. 4b).

Many models have been unable to replicate the timing of rapid ice sheet thinning recorded by the empirical evidence, typically simulating this ice loss approximately 1000-5000 years too early<sup>56,104,105</sup>. The mismatch could be caused by a combination of factors, including uncertainty in the geological boundary conditions and climate forcing, the model resolution and model physics<sup>105–107</sup>, as well as possible error in the empirical data<sup>108</sup>. Reducing data–

model mismatch is necessary for a reliable estimate of ice volume change in Antarctica during the Early and Mid Holocene.

### ***Drivers and controls of rapid ice loss***

The causes of rapid ice loss in the Early-to-Mid Holocene are not yet fully understood (Fig. 5). However, evidence exists for changing oceanographic conditions on the continental shelf, which would have interacted with the ice sheet margin at this time. Intrusions of warm Circumpolar Deep Water occurred in the Amundsen Sea between 10,400 and 8,000 years ago<sup>109</sup>, higher sea surface temperatures are recorded in the Antarctic Peninsula sector at 11,500 to 9,000 and 8,200 to 7,000 years ago<sup>110,111</sup>, and peak sea surface temperatures are recorded off Adélie Land in East Antarctica at ~6,000 years ago<sup>112</sup>. In the Amundsen Sea and Ross Sea, ocean warming is thought to be responsible for thinning of ice shelves and thermal erosion of ice at the grounding line, which accelerated retreat and thinning of the grounded ice sheet<sup>26,35,104,109,113</sup> (Fig. 5b). A positive feedback might have also existed at this time, in which initial ice loss led to a freshening of the ocean surface, reduced Antarctic Bottom Water formation and increased incursions of warm Circumpolar Deep Water<sup>21</sup>. Differences in the timing of oceanic warming around Antarctica might explain why ice loss was asynchronous between sectors during this period; however, insufficient evidence exists to properly assess whether ocean warming was responsible.

Additional factors acting at the ice sheet margin and in the interior likely controlled the exact timing and rate of Early-to-Mid Holocene ice loss. The grounding line in marine-based sectors of the AIS is vulnerable to sea-level change (Fig. 5b), and modelling suggests that sea-level rise sourced from retreating Northern Hemisphere ice sheets might have amplified the rate of Early Holocene ice loss in Antarctica<sup>22</sup>. Bed topography also had an important role. Modelling indicates that episodes of rapid ice loss likely resulted from unstable grounding line retreat across retrograde bed slopes on the continental shelf via a process called marine ice sheet instability<sup>54,82</sup>, and that the timing of retreat might have been delayed by the presence of pinning points and narrow trough geometry<sup>113–115</sup> (Fig. 5b). In the interior, increased snowfall during the Early Holocene might have caused some local thickening of the ice sheet, which would have counteracted and delayed ice thinning until this increased accumulation was outpaced by the dynamic effects from ocean-driven retreat at the margins<sup>30,60</sup>.

### **Inland retreat and readvance**

Following the phase of early rapid ice loss, parts of the AIS grounding line retreated inland of its present-day position, and subsequently readvanced.

### ***Evidence of inland retreat and readvance***

Assessing whether and when the AIS was ever smaller than present during the Holocene is challenging. Evidence for such behaviour can be found within or beneath the present-day ice sheet<sup>116</sup>, or inferred from the response of the solid Earth to retreat and readvance. Currently, however, only limited evidence supports large-scale inland retreat and readvance of the Antarctic grounding line, mostly in the Ross Sea and Weddell Sea sectors.



In the Ross Sea sector, bulk radiocarbon measurements of subglacial sediments from the Siple Coast imply that sites located 200 km upstream of the present-day grounding line were once open to the ocean<sup>29</sup> (Fig. 3). Radiocarbon dates from subglacial sediment collected just inland of the present-day grounding line indicate that inland retreat occurred ~4,800–7,500 years ago<sup>45</sup>. Therefore, readvance to the present-day position must have occurred after this time, broadly corresponding to thickening at the upstream WAIS Divide site (Fig. 2b)<sup>78</sup>. Modelling of subglacial radiocarbon alternatively proposes inland retreat along the Siple Coast at 1,700–4,700 years ago and readvance at 800–1,500 years ago, with the exact timing varying between ice streams<sup>83</sup>.

In the Weddell Sea sector, a substantial dynamic change in the ice sheet occurred during the Holocene<sup>28,117–120</sup>, possibly related to a rapid retreat and then readvance of the grounding line in the vicinity of Robin Subglacial Basin<sup>44</sup> (Fig. 3). Observations of modern bedrock uplift rates in the region cannot be explained by progressive ice loss, and instead might represent a period of rethickening and/or readvance in the Holocene<sup>121</sup>. Ice-penetrating radar data collected at several ice rises in the Weddell Sea embayment suggest a reorganisation of ice flow and possibly inland retreat before re-grounding<sup>28,29,117,120</sup>. The timing of these grounding line changes is uncertain, but inland retreat might have occurred 6,000 years ago, and readvance to the modern position possibly by 3,800 years ago<sup>121,122</sup>. The impact these grounding line fluctuations had on ice volume in the Weddell Sea sector is unclear, as records of ice flow inland indicate that changes were restricted to the coast<sup>123</sup>.

Elsewhere in Antarctica, relative sea level data might record a temporary and small ice mass gain. In the East Antarctica and Antarctic Peninsula sectors, indications exist of mass gain at 7,200 years ago, sometime between 7,100 and 2,700 years ago, and at 700 years ago<sup>48,88,101,124</sup> (Fig. 3), and a number of small-scale readvances of terrestrial and marine ice margins are documented and inferred in several sectors throughout the Mid and Late Holocene<sup>37,67,125–130</sup>. However, these contributions to ice volume change were likely minor.

Available evidence supports retreat of the Antarctic grounding line inland of the present-day position during the Holocene, followed by a readvance, but is currently restricted to the Siple Coast (Ross Sea sector) and Robin Subglacial Basin (Weddell Sea sector) (Figs 3, 5a). How far inland the grounding line retreated, and whether inland retreat and readvance was synchronous between the two sectors, is not yet known. The degree to which widespread Holocene retreat and readvance occurred elsewhere in Antarctica, and the associated impact on total ice volume change, also remains unknown.

### ***Potential drivers of readvance***

Most models that provide insight into the drivers of ice sheet change do not simulate substantial inland retreat and readvance during the Holocene. Ice sheet models do, however, indicate that along the Siple Coast in the Ross Sea and the Robin Subglacial Basin in the Weddell Sea sectors, rethickening and readvance are more likely ice sheet responses than either continued retreat or stable ice thicknesses during the Late Holocene (Fig. 4).

Several explanations for a reversal in the direction of Holocene grounding line migration — from retreat to advance — have been proposed. First, the bed beneath an ice sheet will

rebound following ice mass loss via a process called glacial isostatic adjustment, as recorded in the relative sea-level histories around Antarctica (Fig. 3). Such rebound can lead to the re-grounding of floating ice, potentially slowing down or even reversing grounding line retreat<sup>46,131</sup> (Fig. 5b). Ice sheet and glacial isostatic modelling suggest that the response to past ice loss in the Weddell Sea and Ross Sea sectors can explain the empirical evidence of grounding line readvance and modern uplift rates<sup>29,121</sup>. However, the rate of bed uplift is difficult to estimate, and other models have been unable to replicate rebound-driven readvance<sup>104</sup>. Second, climate variability might have driven inland retreat and readvance. Following a period of prolonged ocean warming<sup>104,109,111</sup>, a switch to ocean cooling could have initiated readvance. This mechanism, potentially associated with atmospheric variability, has been suggested for the Ross Sea sector during the Mid and Late Holocene<sup>83,132</sup>. Glacial isostatic adjustment and/or climate variability could thus have caused a switch from grounding line retreat to readvance in some (or all) sectors during the Holocene, but the dominant driver remains uncertain.

## **Final pre-Industrial ice volume change**

Following the period of widespread rapid ice loss and instances of inland retreat and readvance, the AIS approached its present-day volume in the Late Holocene. Evidence of ice sheet change over the past few millennia enables the observed ice volume trend — which lacks direct measurements prior to the satellite era and particularly prior to the start of the Industrial Era (1850 CE) — to be extended, providing context for modern AIS change.

### ***Ice volume change over recent millennia***

Ice sheet volume was relatively stable during the Late Holocene compared with the changes seen in the Early and Mid Holocene. Rates of ice thickness change drastically reduced after ~4,000 years ago, both near the coast and in the interior (Fig. 2). The grounding line was at or near its modern position in most regions of the continental shelf during the past few millennia, and ice unloading was largely complete, as relative sea level was close to modern levels in most sectors (Fig. 3). Ice sheet models also simulate near-zero mass loss, or slight mass gain, in most sectors over this time (Fig. 4).

Despite the overall picture of ice sheet stability during the Late Holocene, empirical evidence and ice sheet modelling indicate that the ice volume was still changing in some regions of Antarctica. In the east of the Ross Sea sector, >400 m of ice sheet thinning is recorded between 3,200 and 1,900 years ago<sup>53</sup>, and in the west of the sector, 190 m of thinning is recorded between 6,700 and 300 years ago, as well as 25 m of thinning in the past 200 years<sup>54,133</sup>. In East Antarctica, 70 m of thinning and episodes of increased glacier melting are recorded from 4,000 years ago in eastern Dronning Maud Land<sup>27,37</sup>, ice unloading accelerated from 2,700 years ago at Larsemann Hills<sup>48</sup>, and glacial discharge increased from 4,500 years ago in Prydz Bay and from 1,700 years ago in Adélie Land–George V Land<sup>134,135</sup>. Modern observations of bedrock uplift also indicate ice mass loss occurred during the Late Holocene in the vicinity of Totten Glacier, Wilkes Land<sup>130</sup>. Furthermore, ice sheet models simulate continued ice loss into the Late Holocene in East Antarctica, mostly located in Dronning Maud Land, Princess Elizabeth Land and Wilkes Land; although, not all

models agree and limited empirical data are available to confirm this apparent ice loss (Fig. 4).

Centennial-scale fluctuations in glacier extent, glacial discharge and iceberg flux are recorded in the Weddell Sea and Antarctic Peninsula sectors<sup>25,129,136,137</sup> over the Late Holocene, as well as changes in ice shelf geometry<sup>98</sup>. In the Antarctic Peninsula, glacier variability is also indicated after ~2,800 years ago<sup>138,139</sup>: widespread but small-scale readvance is documented from ~400 to 90 years ago<sup>129</sup>, and ice mass loss is inferred from an increased rate of relative sea-level fall 3,100 years ago and ice unloading peaking at ~1,400 and 800 years ago<sup>140,141</sup>. Superimposed on these trends, proxy records from both sides of the Antarctic Peninsula indicate increases in glacial discharge during the past ~500 years, implying that ice volume loss might have continued throughout this period<sup>25,137</sup>. Meanwhile, in the Antarctic interior, thickening likely continued until 1000 years ago<sup>72,78</sup>, after which accumulation generally decreased towards present (Fig. 2b).

All considered, some evidence suggests that local and relatively low magnitude ice volume loss continued to occur in several areas of the AIS during the past few millennia (Fig. 5a). However, it is not clear how the apparent ice loss impacted overall ice sheet volume, or whether this loss outweighed any ice volume gain from rethickening and/or readvance.

### ***Drivers of final pre-Industrial ice volume change***

The low magnitude changes in Antarctic ice volume over the Late Holocene compared with the Early and Mid Holocene imply a weakening of the primary drivers of ice sheet behaviour. Incursions of Circumpolar Deep Water onto the continental shelf decreased in the Amundsen Sea from 7,500 years ago until at least 1,200 years ago<sup>109</sup> and largely ceased in the Ross Sea in the Mid Holocene, possibly following the establishment of a large ice shelf cavity and increased sea ice production<sup>142</sup>. However, high surface and sub-surface ocean temperatures were still present elsewhere on Antarctica's continental shelf during the Late Holocene, and might explain evidence of increased ice loss recorded in East Antarctica and the Antarctic Peninsula<sup>135,143</sup> (Fig. 5). Substantial centennial-scale fluctuations in sea surface temperatures ( $> \pm 1$  °C) occurred in the Antarctic Peninsula sector, with warm events recorded at ~3,500 and between 1,600 and 500 years ago in the west, and since ~500 years ago in the east<sup>110,111</sup>. These events broadly correspond to the periods of ice loss recorded in the sector.

Late Holocene changes in ice sheet volume appear to have been asynchronous across Antarctica, as well as within individual sectors, indicating the likelihood of multiple drivers of ice volume change. Atmospheric forcing might have had a larger influence than oceanic forcing during the Late Holocene (Fig. 5b), although the mechanisms that bring warm air to Antarctica also have a role in triggering warm water intrusions onto the continental shelf and beneath ice shelves. In the Antarctic Peninsula sector, and potentially elsewhere in Antarctica, episodes of local ice loss from ice surface ablation have been linked to an increasing occurrence of La Niña events and enhanced summer insolation<sup>25</sup>, as well as a positive Southern Annular Mode<sup>137,144</sup>, and the regrowth of ice shelves and glacier advances have been associated with periods of synoptic cooling<sup>128,138,145</sup>. Periods of low snow accumulation during the past millennium (between 1250 and 1800 CE) have been associated with reduced solar activity<sup>146</sup> and the cooler atmospheric conditions of the Little

Ice Age<sup>129,147</sup>. A subsequent increase in snow accumulation from 1800 CE into the 20<sup>th</sup> Century has also been attributed to atmospheric circulation change, notably to variations in the Southern Annular Mode<sup>40,148</sup>. The exact contributions of these climatic processes to driving spatially-variable changes in ice volume over recent millennia, as well as the role of natural variability<sup>149</sup>, are not yet fully known.

### ***Stabilisation of the ice sheet***

The AIS was close to its present-day geometry in many regions by the Mid Holocene, but different sectors reached the current configuration at different times. Records from all sectors show that ice surface elevations were close to the modern surface by ~4,000-7,000 years ago<sup>35,58,63,67,150–152</sup>, but continued thinning beyond the Mid Holocene and subsequent rethickening cannot yet be ruled out. In some locations, the present-day ice surface elevation was reached only in the past few millennia, between 3,400 and 200 years ago<sup>37,38,54,61,153</sup>. By contrast, records of the response to ice loading and unloading show little variation through the Late Holocene (Fig. 3), implying stabilisation of the ice sheet geometry. For example, in the northeast of the Antarctic Peninsula, ice unloading was possibly complete by 1,300 years ago<sup>141</sup>, which also broadly corresponds with the stabilisation of some ice shelf extents<sup>67,154</sup>. In the Ross Sea sector, the present-day grounding line position along the Siple Coast and ice shelf extent were likely reached 2,000–3,000 years ago, although some subsequent variability occurred at individual ice streams<sup>142,153,155</sup>. In the Amundsen Sea sector, marine records indicate that the grounding line was stable for ~10,000 years until renewed retreat in the 20<sup>th</sup> Century<sup>156</sup>. Overall, the whole AIS did not reach a stable geometry at a specific time in the Holocene (Fig. 5a), but there is general agreement on the approximate timing within some sectors.

In some localised regions, the ice sheet never reached a stable configuration during the Holocene. High glacial discharge is recorded offshore of East Antarctica and the Antarctic Peninsula from 1,600–2,000 years ago, and has possibly been at unprecedented levels since 1700 CE<sup>134,137</sup>. An increase in the rate of ice unloading is also inferred along the western Antarctic Peninsula over the past 790 years, with ice margin retreat continuing until 1870 CE<sup>138,140</sup>. Accumulation rates near the Antarctic coast and in the Antarctic interior varied throughout the Late Holocene towards the present day, and show a general increase to modern rates since 1800 CE<sup>40,147</sup>. Although limited evidence exists to support continuous and Antarctic-wide ice volume change, ice loss did occur in at least some regions into the Industrial era.

### **Contribution to global sea-level change**

A direct consequence of Antarctic ice sheet change is global sea-level change. However, disentangling the signal of the AIS from other sources of sea-level change is challenging.

Relatively rapid GMSL rise occurred in the Early-to-Mid Holocene (Fig. 1), implying a period of unstable ice loss from global ice sheets. Between the onset of the Holocene and 6,700 years ago — when retreat of the Laurentide, Greenland and Eurasian ice sheets in the Northern Hemisphere had ceased<sup>157–160</sup> — GMSL rose by ~58 m<sup>16</sup>. The Northern

Hemisphere ice sheets contributed approximately 46 m to GMSL during this time window, leaving 12 m to be sourced from Antarctica<sup>161</sup>. However, determining the exact ice sheet contributions is difficult, and these estimates depend on an uncertain sea-level budget at the Last Glacial Maximum<sup>16,162,163</sup>. Based on model simulations of the AIS (Fig. 4), Antarctica contributed only 2.4–6.9 m to GMSL between the start of the Holocene and 6,700 years ago.

Numerical modelling indicates that the AIS could have increased relative sea levels by up to 5 m over 4,000 years during the period of rapid ice loss, which is predicted mostly in the north and central Pacific Ocean, northwest Atlantic Ocean, and central Indian Ocean (Fig. 6a; Supplementary Information). Rapid relative sea-level rise in the Early-to-Mid Holocene is recorded by empirical data in Southeast Asia, the Caribbean, the northwest and northeast Atlantic Ocean, the southern African coast, and the western Pacific Ocean<sup>164–170</sup>, which is consistent with a substantial contribution from Antarctica over this time.

A progressive decrease in the rate of GMSL change followed in the Mid-to-Late Holocene (Fig. 1). Approximately 3.8 m of GMSL rise has occurred since 6,700 years ago, most likely sourced from Antarctica and mountain glaciers<sup>16,161,171</sup>. Based on model simulations of the AIS (Fig. 4), Antarctica contributed somewhere between -0.2 m and 5.3 m to GMSL over the past 6,700 years. A major Antarctic contribution (>1 m) to GMSL might have ceased by 6,000 years ago<sup>172–174</sup>, or continued until 4,000 years ago<sup>175–180</sup> or 2,000–1,000 years ago<sup>16,164,171,181,182</sup>. If the AIS underwent a period of readvance and ice volume gain in the Mid-to-Late Holocene, a widespread drop in sea level (up to 35 cm) should have occurred, mainly in the north and central Pacific Ocean, and sea-level rise (up to 50 cm) would have been restricted to the Southern Ocean (Fig. 6b; Supplementary Information). This widespread sea-level fall in the Mid-to-Late Holocene could have been up to 120 cm, simulated using the model with greatest ice volume gain, but the substantial interior ice sheet thickening simulated in this model needs corroboration from empirical evidence (Supplementary Fig. 1).

Although evidence exists for continued relative sea-level rise in some mid latitude locations<sup>167,183–186</sup>, sea level reconstructions from Southeast Asia, the Indian Ocean, and the equatorial and southwest Pacific Ocean record a trend of relative sea-level fall in the Late Holocene<sup>172,182,187–190</sup>. This fall is primarily due to time-decaying sea level processes<sup>191</sup>, but the pattern is also broadly consistent with a period of Antarctic ice volume gain. Tighter constraints on temporal variations in Late Holocene relative sea level<sup>188,192</sup> are required to determine whether a component of the recorded change is related to AIS volume change.

Differences between estimates of GMSL and global ice volume change still need to be resolved. Notably, the AIS contributed 2.4–6.9 m to a period of rapid GMSL rise in the Early-to-Mid Holocene based on AIS model simulations, but possibly up to 12 m based on the Northern Hemisphere ice sheet contributions. Similarly, the AIS likely became the largest source of GMSL rise after 6,700 years ago; however, determining whether the AIS contribution to GMSL through the Late Holocene was greater than that of mountain glacier or steric changes is not yet possible.

The rate, magnitude and geographic distribution of future sea-level change depends on how the AIS will respond to climate change<sup>193</sup>. In the Holocene, AIS volume responded on a range of temporal (10s–1000s years) and spatial (between and within ice sheet sectors)

scales — including some regions switching from volume loss to volume gain — which likely resulted in a complex and temporally varying pattern of global sea-level change (Fig. 6). Accurately predicting the spatial distribution of ice volume change and, therefore, the net Antarctic contribution to sea-level change — both in the Holocene and in the future — relies on several factors (for example, solid Earth, oceanographic and atmospheric processes) which are not adequately known<sup>193–195</sup>.

## Summary and future perspectives

The geometry of the AIS did not remain stable throughout the Holocene, and periods of rapid ice volume change are likely to have affected global sea level.

The causes of AIS volume change in the Holocene (Fig. 5) provide insight into the processes that are driving current and anticipated future ice sheet behaviour. Similar to that observed in parts of Antarctica today, grounded ice loss in the Holocene was likely driven by incursions of warm Circumpolar Deep Water on the continental shelf and subsequent thinning of ice shelves<sup>7,196</sup>. Present-day grounding line retreat and ice sheet thinning is predicted to accelerate due to marine ice sheet instability<sup>13,197–199</sup>, and evidence exists that this process also occurred in the Holocene. Certain topographic settings were able to initially delay or slow retreat in the Holocene but, once a threshold was reached, accelerated ice loss was able to persist for many centuries. Although, in some cases, this retreat was reversed. In the past 20 years, a speedup of grounded ice flow has been observed following the disintegration of ice shelves<sup>200,201</sup>. Such behaviour appears to be unprecedented when compared with Holocene records of ice shelf change<sup>98,145,202</sup>. Increased snowfall occurred in Antarctica during the 20<sup>th</sup> Century, and continued accumulation increases have the potential to partly offset ice volume loss into the future as the atmosphere warms<sup>148,203</sup>. A coupling between snow accumulation and atmospheric temperature similarly existed throughout much of the Holocene<sup>77</sup>, although how much the increase in accumulation contributed to ice volume change, and whether this was able to offset retreat and thinning near the ice sheet margins, is currently difficult to estimate.

The picture of the AIS during the Holocene remains incomplete. First, evidence of past ice thickness change, grounding line migration or the response to ice loading is entirely lacking across vast regions, and many regions have only sparse evidence. Limited information is available for long stretches of the ice sheet margin in East Antarctica, where several glaciers (for example, Totten, Denman and Vanderford) are changing dramatically today<sup>2</sup>. Similarly, much of the Antarctic interior has inadequate data, and changes in ice thickness currently are only inferred from widely scattered ice core records. Furthermore, large areas of the continental shelf in the Ross Sea, Weddell Sea and Lambert-Amery system are unstudied, largely due to the presence of ice shelves and sea ice which hamper the collection of marine sediment cores. In addition to more data collection, some of these gaps could be filled through application of new techniques. For example, measurements of internal ice layers can be utilised to constrain ice volume changes across much of the ice sheet interior<sup>204</sup>, and subglacial sediment and bedrock cores can be used to test whether and when inland retreat occurred<sup>29,205</sup>.

Second, accurate reconstructions of past ice sheet change are dependent on chronological control, which has an inherent uncertainty, but also errors that can be difficult to quantify. For example, determining the timing of ice thickness change from cosmogenic exposure dating is dependent on the nuclide production rate (that varies in space and time<sup>108,206</sup>), which currently lacks Antarctic calibration. Meanwhile, the timing of grounding line retreat from radiocarbon dating is dependent on a range of factors including the preservation of calcareous fossils, which provide the most robust retreat ages, and a marine reservoir correction that is often approximated from an Antarctic-wide average owing to a paucity of regional data<sup>207,208</sup>. Developments in these chronological techniques, such as ramped-pyrolysis and compound-specific radiocarbon dating<sup>59,209</sup> and cosmogenic *in-situ* carbon-14 exposure dating<sup>210,211</sup>, as well as better quantification of uncertainties, will improve understanding of the leads and lags of ice sheet change.

Third, the drivers of ice volume change and the contribution to GMSL remain poorly known. These knowledge gaps can be investigated with ice sheet and sea level modelling, however disagreements currently exist between model simulations and empirical data, as well as between models. Improved accuracy of ice sheet model simulations will be achieved by: testing against empirical data<sup>31–33,204</sup>; better representation of bed topography and ice sheet processes in models<sup>1,212</sup>; and coupling to other Earth-System models that incorporate sea level and climate feedbacks, and that account for lateral variations in Earth rheology<sup>21,22,46,213,214</sup>. Despite advances in the understanding of ice–Earth feedbacks and past atmosphere and ocean conditions<sup>46,215</sup>, information on the underlying mantle viscosity in Antarctica is scarce<sup>46,216,217</sup>, and records of Holocene environmental change are limited, particularly reconstructions of ocean temperature<sup>109–111</sup>. Additionally, constraining AIS change via the interpretation of sea-level change in the mid-to-low latitudes requires the quantification of lower mantle viscosity as well as improved reconstructions of non-Antarctic ice sheet histories<sup>16,161,180</sup>.

In summary, many of the changes in the AIS during the Holocene were similar to changes anticipated for the coming centuries. However, further progress in our understanding of ice sheet change in the Holocene is urgently needed to provide useful bounds on the potential rate and duration of ice sheet loss, and possible regrowth, and to advance our knowledge of the processes that might enhance or reduce Antarctica's future contribution to sea-level rise.

## Display items

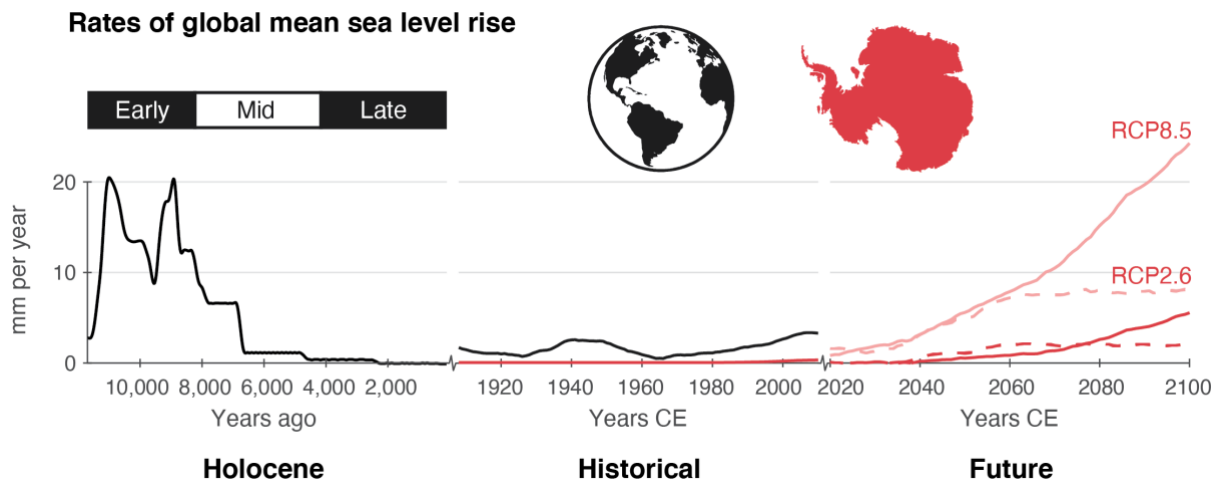
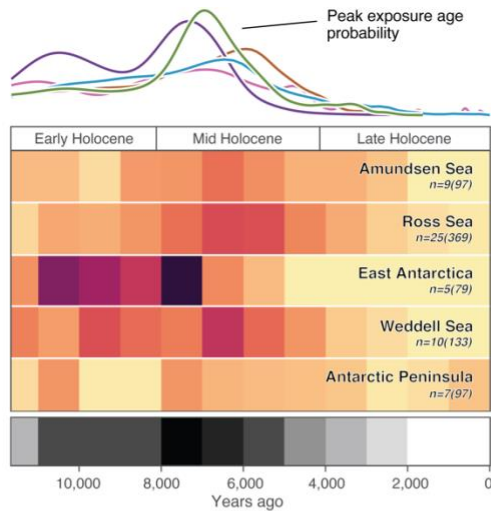
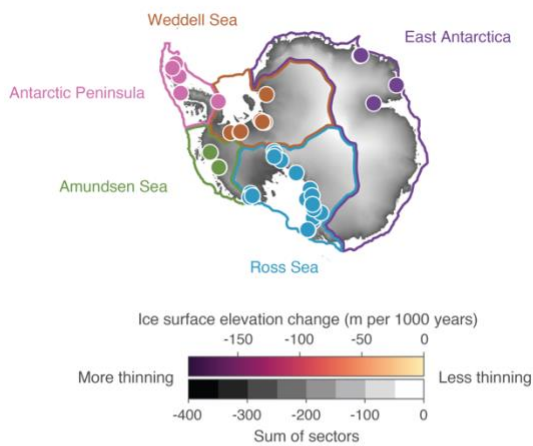


**Figure 1. Past, present and future sea-level change.** Mean rates of sea-level rise for the Early (11,700–8,200 years ago), Mid (8,200–4,200 years ago) and Late (4,200 years ago to 1850 CE) Holocene<sup>16</sup>, historical observations since 1900 CE<sup>11</sup>, and future projections to 2100 CE<sup>12</sup>. The global total is shown in black and the Antarctic contribution in red. Future projections are for RCP2.6/SSP1-26 (dashed lines) and RCP8.5/SSP5-85 (solid lines) emission scenarios, and include only the Antarctic-specific contribution. The darker and paler sets of red lines are for the main and risk-averse projections<sup>12</sup>, respectively, and the difference reflects uncertainty in the processes controlling Antarctic ice volume loss. The contribution of the Antarctic Ice Sheet to sea-level change in the Holocene is not known, motivating an evaluation of the ice volume change over this time.



**a Ice thickness from cosmogenic exposure data**



**b Ice thickness from ice core data**

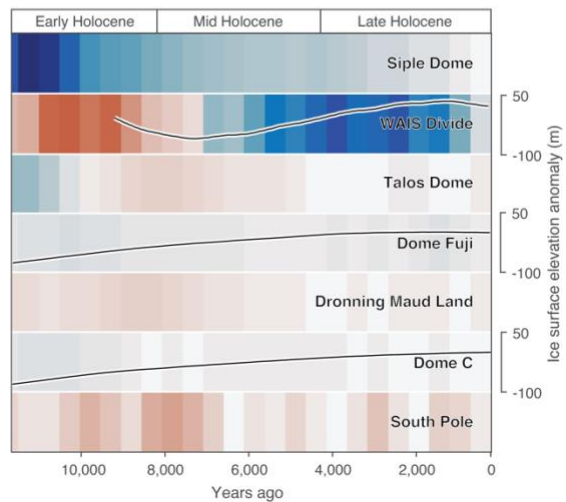
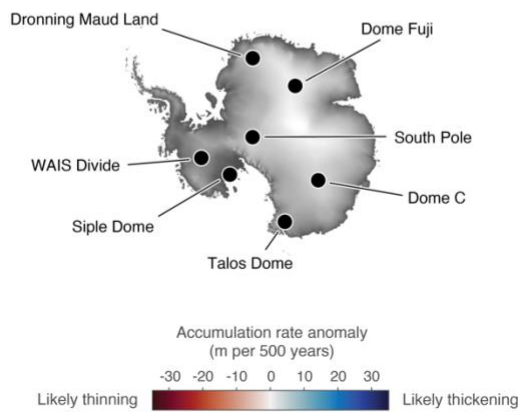


**Figure 2. Records of Holocene ice thickness change.** **a** | The relative probability of rock exposure and the corresponding change in ice surface elevation for different sectors of Antarctica as determined from cosmogenic exposure data. Data are sourced from the ICE-D Antarctica database<sup>218</sup>, and filtered and analysed as described in the Supplementary Information. Note, these estimates reflect changes at the margin, where thinning was greatest, and do not reflect sector-wide thinning rates. **b** | The accumulation rate and corresponding change in ice surface elevation from ice core data. Records were included where the accumulation rate spanned the length of the Holocene<sup>39</sup>, and are displayed relative to pre-Industrial (1700–1850 CE). Black lines for WAIS Divide, Dome C and Dome Fuji represent inversion-derived ice surface elevation changes<sup>72,78</sup>. The timings of the Early, Mid and Late Holocene are defined in Fig. 1. Ice sheet thinning near the margin is principally recorded between 11,000 and 5,000 years ago, and some ice thickening occurred across most of the interior since the Early Holocene.

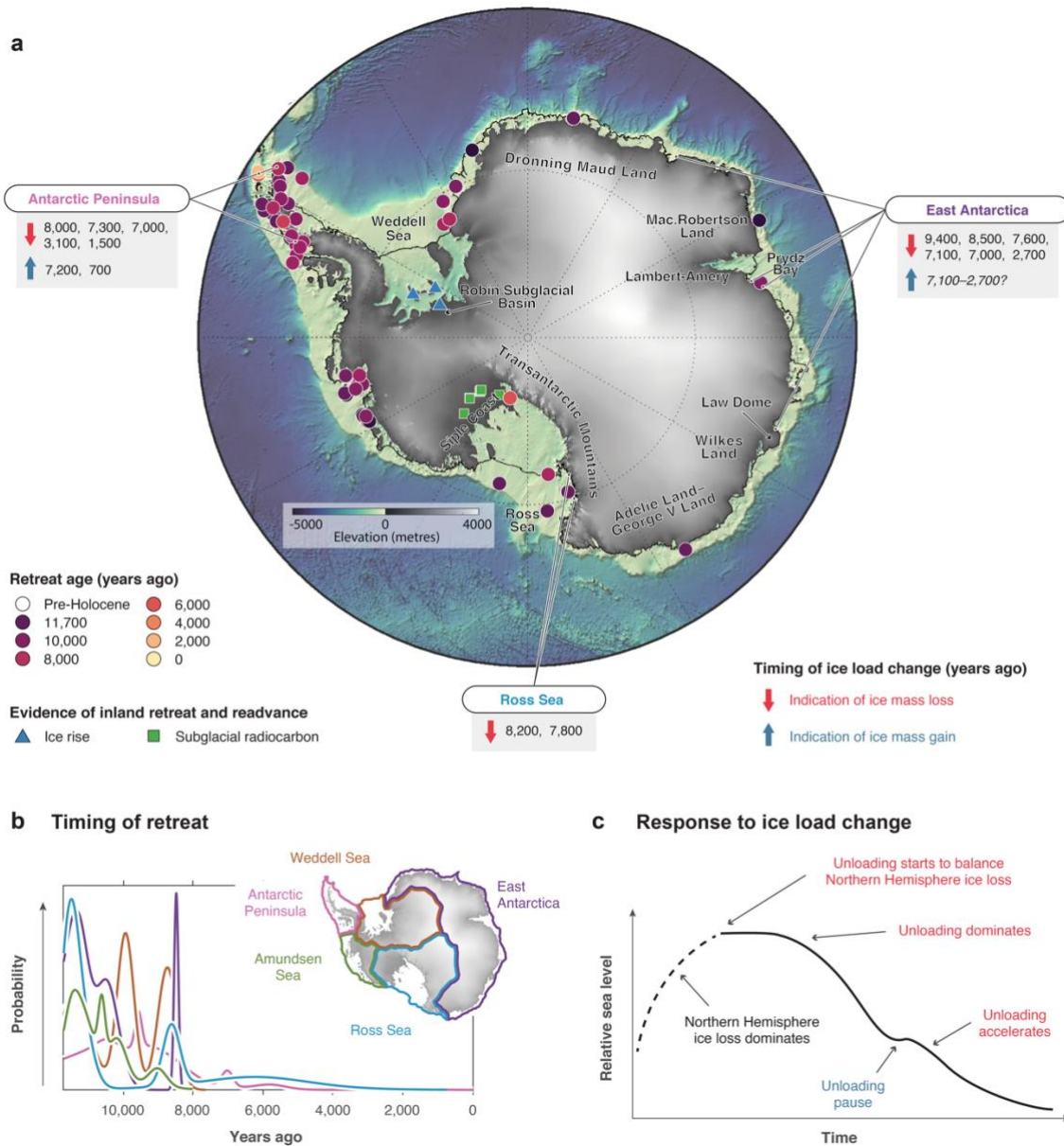
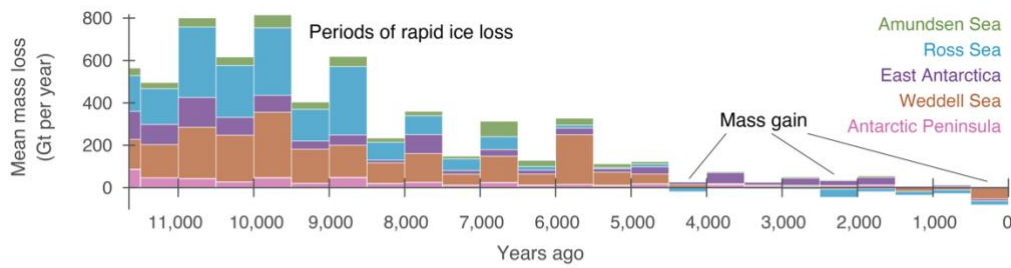


**Figure 3. Records of grounding line migration and response to ice load change. a)** Present-day grounded ice extent, ages of past grounding line retreat across the continental shelf<sup>41,42,45,81,82,90,92–94,96–98,138,219–222</sup>, and locations of inland retreat and readvance<sup>29,44</sup>. Indications of ice mass loss and gain are illustrated as red and blue arrows, respectively, based on interpretations of relative sea level records at sites around the Antarctic margin (as outlined in part c)<sup>47,48,84,87–89,91,100,101,223</sup>. **b)** Probability distributions of retreat ages, incorporating the 2-sigma uncertainties, for each sector (described in the Supplementary Information). **c)** Schematic of the typical trend of relative sea-level change in Antarctica; the local signal of ice unloading first starts to balance the signal of Northern Hemisphere ice loss, and then dominates and accelerates, and in some cases pauses, towards present. The timings of these relative sea-level changes provide an indication of when ice mass loss (red) or gain (blue) occurred. Note, the Amundsen Sea sector has limited constraints<sup>224</sup> and the Weddell Sea sector has no constraints on the Holocene response to ice unloading. Most grounding line retreat had occurred by 8,000 years ago, and evidence exists of subsequent

readvance in the Ross Sea and Weddell Sea sectors. Elsewhere, relative sea level records mostly indicate ice mass loss at times from 9,400 to 1,500 years ago.

**a Modelled mass change**



**b Modelled thickness change**

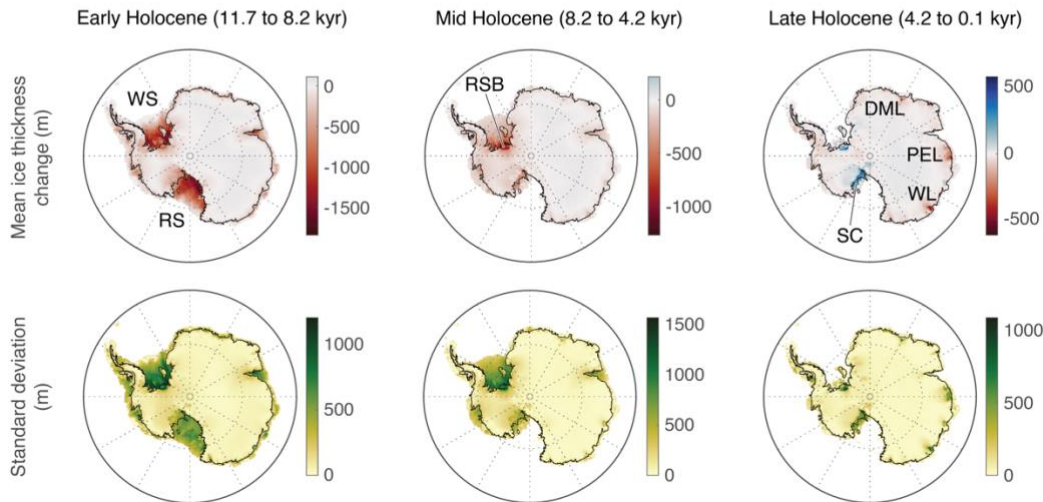


**Figure 4. Modelled ice volume change in the Holocene.** **a** Mean mass loss of grounded ice from 11 ice sheet models in 500-year bins for each sector. Negative mass loss indicates mass gain. The models used are the best-fit<sup>22,31–34</sup>, ensemble mean<sup>21</sup> or reference simulation<sup>29,102,103</sup> from each modelling study, and include the two endmember models from ref.<sup>22</sup> and the two solid-Earth scenarios from ref.<sup>34</sup>. **b** Mean (top) and standard deviation (bottom) of ice thickness change across the models for the Early, Mid and Late Holocene. The present-day grounding line is in black. Note, the extent of possible ice sheet readvance in the Ross Sea and Weddell Sea sectors is likely underestimated as most models do not simulate extensive inland retreat, and the reference simulation from ref.<sup>29</sup> prioritises the potential for inland retreat rather than subsequent readvance. Additionally, cosmogenic exposure data indicate that the periods of rapid ice loss likely occurred 1,000–5,000 years later than the models indicate. The models simulate periods of rapid ice volume loss in the Early and Mid Holocene, mostly in the Ross Sea and Weddell Sea sectors, with some ice volume gain occurring in the Late Holocene. WS, Weddell Sea; RS, Ross Sea; RSB, Robin Subglacial Basin; SC, Siple Coast; DML, Dronning Maud Land; PEL, Princess Elizabeth Land; WL, Wilkes Land.

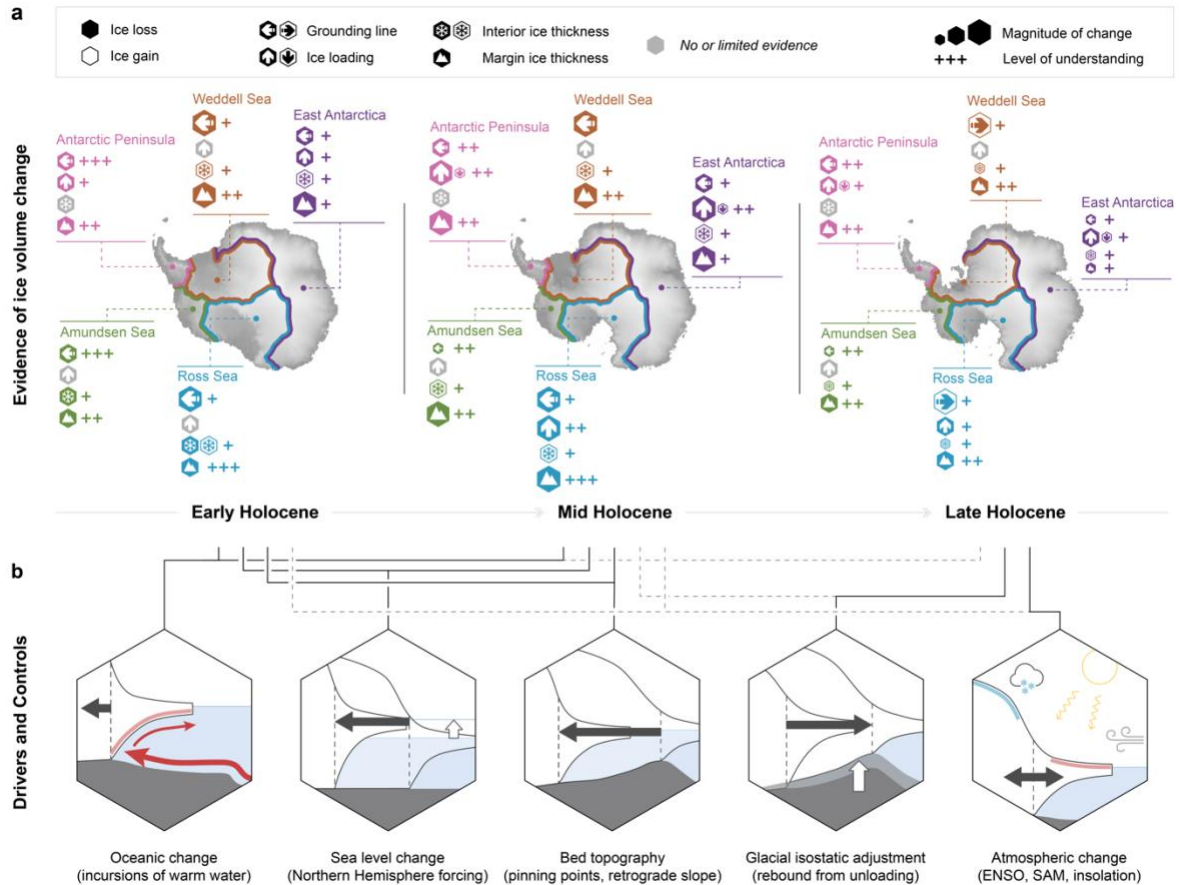


**Figure 5. Overview of Antarctic Ice Sheet change in the Holocene.** **a**) Evidence of ice volume loss and gain for each ice sheet sector during the Early, Mid and Late Holocene. The magnitude and level of understanding of these changes are relative measures for the Holocene, based on the evidence discussed in this review. Interior ice thickness change represents evidence from ice cores, and margin ice thickness change represents evidence from cosmogenic exposure age data, which are mostly located nearer to the ice sheet margin. The background map of Antarctica is the ice sheet geometry from the mean of the models in Fig. 4 at the start of each period. **b**) Primary drivers and controls of ice sheet volume change during the Early, Mid and Late Holocene. The dashed vertical line in the cross-section diagrams represents the ice thickness at the grounding line, which retreats or advances in the direction of the black arrow. ENSO, El Niño-Southern Oscillation (La Niña); SAM, Southern Annular Mode.

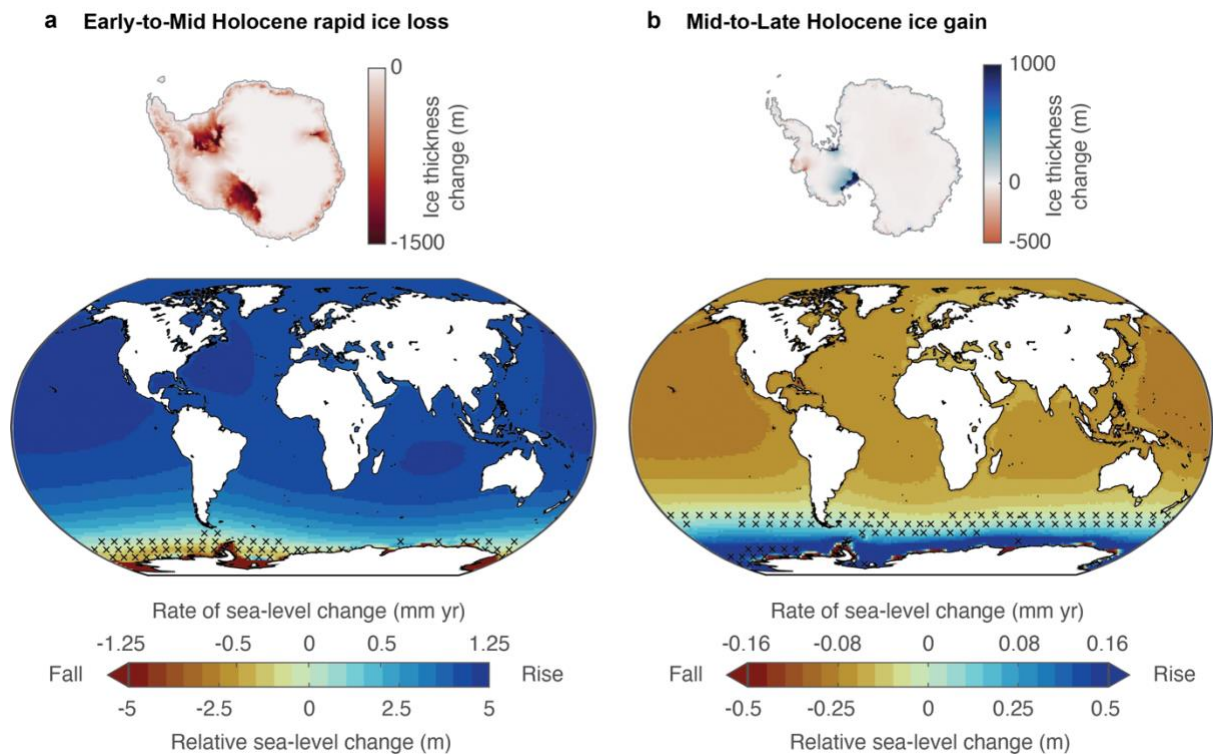


**Figure 6. Patterns of global sea-level change due to Holocene Antarctic ice volume change.** **a|** Scenario of rapid ice loss in the Early-to-Mid Holocene. Ice thickness change is derived from the mean of 11 ice sheet models (Fig. 4) from 12,000 to 8,000 years ago, but the empirical evidence indicates that this period of rapid ice loss possibly occurred later. The largest sea-level rise is predicted in the north and central Pacific Ocean, northwest Atlantic Ocean, and central Indian Ocean. **b|** Scenario of ice volume gain, possibly in the Late Holocene. Ice thickness change is derived from the ice sheet model with the greatest ice sheet readvance<sup>29</sup>, simulated between 3,000 years ago and present. The largest sea-level fall (up to 0.35 m) is predicted in the north and central Pacific Ocean, and sea-level rise is predicted in the Southern Ocean. When using the model with greatest ice volume gain, opposed to just readvance, sea-level fall up to 1.2 m is predicted (Supplementary Fig. S1). Sea level modelling was carried out for these scenarios using a range of Earth models, and is described in the Supplementary Information. The cross stippling indicates where the signal is insignificant (mean predicted relative sea-level change is less than the standard deviation from 24 Earth models). The displayed rates of sea-level change are averages for the time period, and more extreme rates would have occurred within these periods.

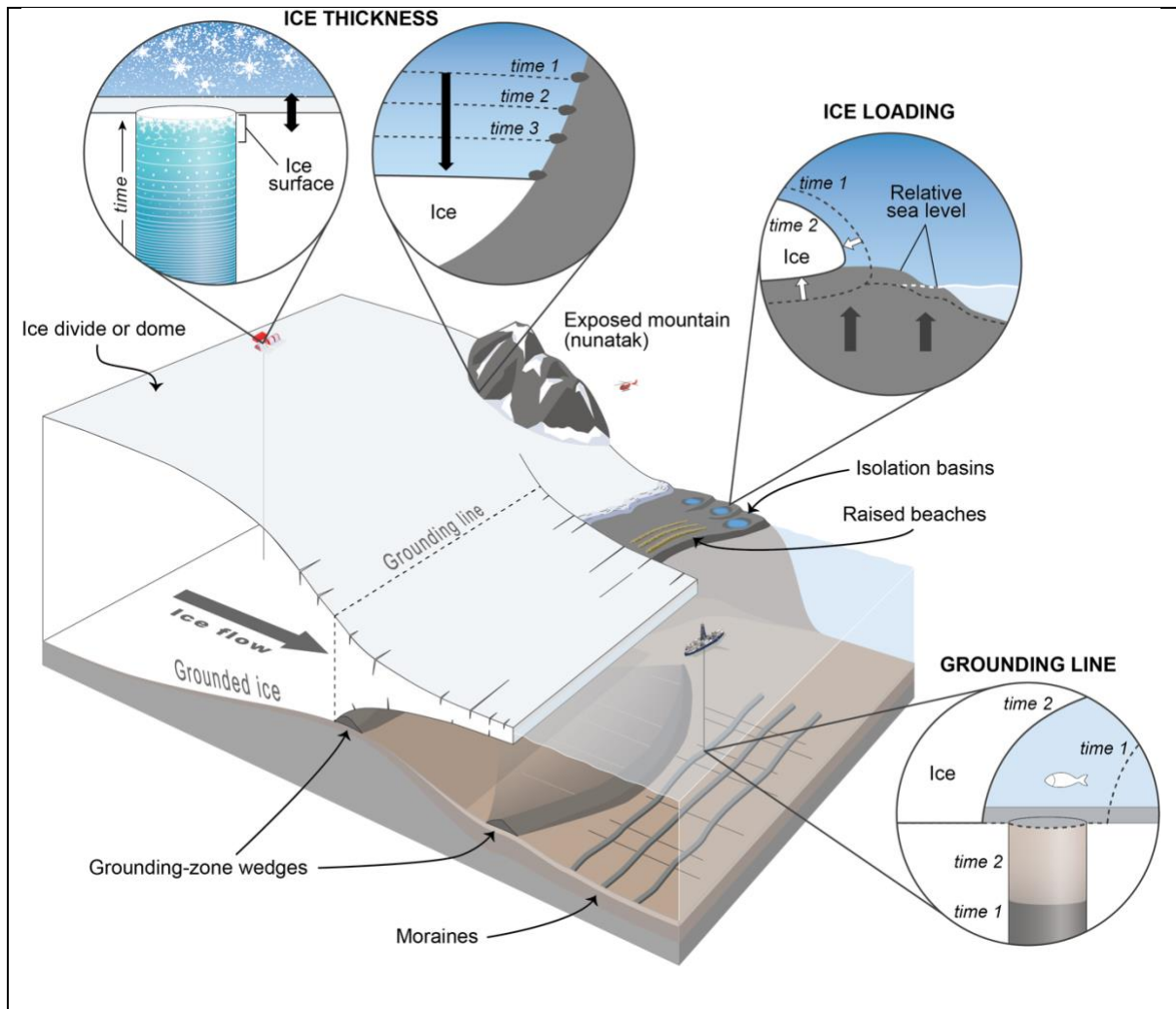
## Box 1: Reconstructing ice volume change

The common approaches used to determine past changes in ice sheet volume are:

**Ice thickness change:** Cosmogenic exposure dating is applied in mountainous locations that are ice-free today. The method exploits the accumulation of cosmogenic nuclides in boulder and bedrock surfaces to determine the time at which a location was exposed by a receding ice margin<sup>225</sup>. A timeline of ice surface lowering, implying ice sheet thinning, is derived by sampling rock surfaces in elevation transects that extend up from the modern ice margin<sup>49,53</sup>. In the ice sheet interior, regional snow accumulation is the primary control on ice surface elevation change<sup>226</sup>. Snow accumulation rates derived from ice cores therefore provide a useful indicator of past ice thickness change. Inverse modelling<sup>72,78</sup> and ice core analysis of the total air-content and water isotope ratio<sup>39,227</sup> can also provide estimates of the past ice surface elevation, but most reconstructions have focused on the Last Glacial Maximum rather than the Holocene.

**Grounding line migration:** Past retreat of the grounding line is recorded by grounding-zone wedges, moraines and other subglacial bedforms on the seafloor of the continental shelf<sup>228</sup>. Sediment cores are collected from these depositional features to determine the timing of retreat. Radiocarbon dating is typically applied to the contact between subglacial and glacial marine sediment, and ages often represent a minimum timing because dating is carried out on organic glacial marine material that is deposited after grounding line retreat<sup>41,81</sup>.

**Response to ice load change:** Ice sheets load the underlying crust, causing an isostatic lowering of the bed that is approximately proportional to the ice mass, with the absolute magnitude depending on local Earth rheology<sup>46</sup>. When this ice mass is reduced, isostatic uplift occurs and the bed rebounds. Coastal locations record this loading and unloading signal of regional ice mass change as a raising and lowering of relative sea level. This signal can be reconstructed by dating material from sites such as isolation basins, raised beaches and lake deltas, which record former sea level positions<sup>47,101,229</sup>.



## Data availability

The data shown in Figures 1, 2, 3, 4 and 6, and the code used to analyse the data and generate the figures can be found at <https://github.com/rs-jones/antarctica-holocene>.



## References

1. Morlighem, M. *et al.* Deep glacial troughs and stabilizing ridges unveiled beneath the margins of the Antarctic ice sheet. *Nat. Geosci.* **13**, 132–137 (2020).
2. Rignot, E. *et al.* Four decades of Antarctic Ice Sheet mass balance from 1979–2017. *Proc. Natl. Acad. Sci.* **116**, 1095–1103 (2019).
3. Konrad, H. *et al.* Net retreat of Antarctic glacier grounding lines. *Nat. Geosci.* **11**, 258 (2018).
4. McMillan, M. *et al.* Increased ice losses from Antarctica detected by CryoSat-2. *Geophys. Res. Lett.* **41**, 3899–3905 (2014).
5. Smith, B. *et al.* Pervasive ice sheet mass loss reflects competing ocean and atmosphere processes. *Science* **368**, 1239–1242 (2020).
6. Pritchard, H. *et al.* Antarctic ice-sheet loss driven by basal melting of ice shelves. *Nature* **484**, 502–505 (2012).
7. Paolo, F. S., Fricker, H. A. & Padman, L. Volume loss from Antarctic ice shelves is accelerating. *Science* **348**, 327–331 (2015).
8. Alley, R. B. *et al.* Oceanic forcing of ice-sheet retreat: West Antarctica and more. *Annu. Rev. Earth Planet. Sci.* **43**, 207–231 (2015).
9. Rosier, S. H. *et al.* The tipping points and early-warning indicators for Pine Island Glacier, West Antarctica. *The Cryosphere* 1–23 (2021) doi:10.5194/tc-2020-186.
10. Meredith, M. *et al.* Polar Regions. in *IPCC Special Report on the Ocean and Cryosphere in a Changing Climate* (eds. Pörtner, H. O. *et al.*) 203–320 (2019).
11. Frederikse, T. *et al.* The causes of sea-level rise since 1900. *Nature* **584**, 393–397 (2020).
12. Edwards, T. L. *et al.* Projected land ice contributions to twenty-first-century sea level rise. *Nature* **593**, 74–82 (2021).
13. DeConto, R. M. *et al.* The Paris Climate Agreement and future sea-level rise from Antarctica. *Nature* **593**, 83–89 (2021).
14. Oppenheimer, M. *et al.* Sea Level Rise and Implications for Low-Lying Islands, Coasts and Communities. in *IPCC Special Report on the Ocean and Cryosphere in a Changing Climate* (eds. Pörtner, H. O. *et al.*) (2019).
15. Kopp, R. E. *et al.* Temperature-driven global sea-level variability in the Common Era. *Proc. Natl. Acad. Sci.* **113**, E1434–E1441 (2016).
16. Lambeck, K., Rouby, H., Purcell, A., Sun, Y. & Sambridge, M. Sea level and global ice volumes from the Last Glacial Maximum to the Holocene. *Proc. Natl. Acad. Sci.* 201411762 (2014).
17. Goelzer, H., Coulon, V., Pattyn, F., de Boer, B. & van de Wal, R. Brief communication: On calculating the sea-level contribution in marine ice-sheet models. *The Cryosphere* **14**, 833–840 (2020).
18. Weertman, J. Stability of the Junction of an Ice Sheet and an Ice Shelf. *J. Glaciol.* **13**, 3–11 (1974).
19. Bentley, M. J. *et al.* A community-based geological reconstruction of Antarctic Ice Sheet deglaciation since the Last Glacial Maximum. *Quat. Sci. Rev.* **100**, 1–9 (2014).
20. Weber, M. *et al.* Millennial-scale variability in Antarctic ice-sheet discharge during the last deglaciation. *Nature* **510**, 134–138 (2014).
21. Golledge, N. R. *et al.* Antarctic contribution to meltwater pulse 1A from reduced Southern Ocean overturning. *Nat. Commun.* **5**, 1–10 (2014).

22. Gomez, N., Weber, M. E., Clark, P. U., Mitrovica, J. X. & Han, H. K. Antarctic ice dynamics amplified by Northern Hemisphere sea-level forcing. *Nature* **587**, 600–604 (2020).
23. Carlson, A. E. & Clark, P. U. Ice sheet sources of sea level rise and freshwater discharge during the last deglaciation. *Rev. Geophys.* **50**, RG4007 (2012).
24. Rohling, E. J. *et al.* Differences between the last two glacial maxima and implications for ice-sheet,  $\delta^{18}\text{O}$ , and sea-level reconstructions. *Quat. Sci. Rev.* **176**, 1–28 (2017).
25. Pike, J., Swann, G. E. A., Leng, M. J. & Snelling, A. M. Glacial discharge along the west Antarctic Peninsula during the Holocene. *Nat. Geosci.* **6**, 199–202 (2013).
26. Yokoyama, Y. *et al.* Widespread collapse of the Ross Ice Shelf during the late Holocene. *Proc. Natl. Acad. Sci.* **113**, 2354–2359 (2016).
27. Sproson, A. D. *et al.* Beryllium isotopes in sediments from Lake Maruwan Oike and Lake Skallen, East Antarctica, reveal substantial glacial discharge during the late Holocene. *Quat. Sci. Rev.* **256**, 106841 (2021).
28. Brisbourne, A. M. *et al.* Constraining Recent Ice Flow History at Korff Ice Rise, West Antarctica, Using Radar and Seismic Measurements of Ice Fabric. *J. Geophys. Res. Earth Surf.* **124**, 175–194 (2019).
29. Kingslake, J. *et al.* Extensive retreat and re-advance of the West Antarctic ice sheet during the Holocene. *Nature* **558**, 430–434 (2018).
30. King, C., Hall, B., Hillebrand, T. & Stone, J. Delayed maximum and recession of an East Antarctic outlet glacier. *Geology* **48**, 630–634 (2020).
31. Albrecht, T., Winkelmann, R. & Levermann, A. Glacial-cycle simulations of the Antarctic Ice Sheet with the Parallel Ice Sheet Model (PISM) – Part 2: Parameter ensemble analysis. *The Cryosphere* **14**, 633–656 (2020).
32. Briggs, R. D., Pollard, D. & Tarasov, L. A data-constrained large ensemble analysis of Antarctic evolution since the Eemian. *Quat. Sci. Rev.* **103**, 91–115 (2014).
33. Whitehouse, P. L., Bentley, M. J. & Le Brocq, A. M. A deglacial model for Antarctica: geological constraints and glaciological modelling as a basis for a new model of Antarctic glacial isostatic adjustment. *Quat. Sci. Rev.* **32**, 1–24 (2012).
34. Pollard, D., Gomez, N. & Deconto, R. M. Variations of the Antarctic Ice Sheet in a Coupled Ice Sheet-Earth-Sea Level Model: Sensitivity to Viscoelastic Earth Properties. *J. Geophys. Res. Earth Surf.* **122**, 2124–2138 (2017).
35. Johnson, J. S. *et al.* Deglaciation of Pope Glacier implies widespread early Holocene ice sheet thinning in the Amundsen Sea sector of Antarctica. *Earth Planet. Sci. Lett.* **548**, 116501 (2020).
36. Jones, R. S. *et al.* Regional-scale abrupt Mid-Holocene ice sheet thinning in the western Ross Sea, Antarctica. *Geology* **49**, 278–282 (2020).
37. Kawamata, M. *et al.* Abrupt Holocene ice-sheet thinning along the southern Soya Coast, Lützow-Holm Bay, East Antarctica, revealed by glacial geomorphology and surface exposure dating. *Quat. Sci. Rev.* **247**, 106540 (2020).
38. Spector, P. *et al.* Rapid early-Holocene deglaciation in the Ross Sea, Antarctica. *Geophys. Res. Lett.* **44**, 7817–7825 (2017).
39. Buizert, C. *et al.* Antarctic surface temperature and elevation during the Last Glacial Maximum. *Science* **372**, 1097–1101 (2021).
40. Thomas, E. R. *et al.* Regional Antarctic snow accumulation over the past 1000 years. *Clim. Past* **13**, 1491–1513 (2017).
41. Prothro, L. O. *et al.* Timing and pathways of East Antarctic Ice Sheet retreat. *Quat. Sci. Rev.* **230**, 106166 (2020).

42. Smith, J. A. *et al.* New constraints on the timing of West Antarctic Ice Sheet retreat in the eastern Amundsen Sea since the Last Glacial Maximum. *Glob. Planet. Change* **122**, 224–237 (2014).
43. Mackintosh, A. *et al.* Retreat of the East Antarctic ice sheet during the last glacial termination. *Nat. Geosci.* **4**, 195–202 (2011).
44. Siegert, M. J. *et al.* Major Ice Sheet Change in the Weddell Sea Sector of West Antarctica Over the Last 5,000 Years. *Rev. Geophys.* **57**, 1197–1223 (2019).
45. Venturelli, R. A. *et al.* Mid-Holocene Grounding Line Retreat and Readvance at Whillans Ice Stream, West Antarctica. *Geophys. Res. Lett.* **47**, e2020GL088476 (2020).
46. Whitehouse, P. L., Gomez, N., King, M. A. & Wiens, D. A. Solid Earth change and the evolution of the Antarctic Ice Sheet. *Nat. Commun.* **10**, 1–14 (2019).
47. Hall, Baroni, C. & Denton, G. H. Holocene relative sea-level history of the Southern Victoria Land Coast, Antarctica. *Glob. Planet. Change* **42**, 241–263 (2004).
48. Hodgson, D. A. *et al.* Rapid early Holocene sea-level rise in Prydz Bay, East Antarctica. *Glob. Planet. Change* **139**, 128–140 (2016).
49. Small, D., Bentley, M. J., Jones, R. S., Pittard, M. L. & Whitehouse, P. L. Antarctic ice sheet palaeo-thinning rates from vertical transects of cosmogenic exposure ages. *Quat. Sci. Rev.* **206**, 65–80 (2019).
50. Ackert, R. P. *et al.* Measurements of past ice sheet elevations in interior West Antarctica. *Science* **286**, 276–280 (1999).
51. Lindow, J. *et al.* Glacial retreat in the Amundsen Sea sector, West Antarctica – first cosmogenic evidence from central Pine Island Bay and the Kohler Range. *Quat. Sci. Rev.* **98**, 166–173 (2014).
52. Johnson, J. S. *et al.* Rapid thinning of Pine Island Glacier in the early Holocene. *Science* **343**, 999–1001 (2014).
53. Stone, J. O. *et al.* Holocene deglaciation of Marie Byrd land, west Antarctica. *Science* **299**, 99–102 (2003).
54. Jones, R. *et al.* Rapid Holocene thinning of an East Antarctic outlet glacier driven by marine ice sheet instability. *Nat. Commun.* **6**, 8910 (2015).
55. Goehring, B. M., Balco, G., Todd, C., Moening-Swanson, I. & Nichols, K. Late-glacial grounding line retreat in the northern Ross Sea, Antarctica. *Geology* **47**, 291–294 (2019).
56. Stutz, J. *et al.* Mid-Holocene thinning of David Glacier, Antarctica: Chronology and Controls. *The Cryosphere* **15**, 5447–5471 (2021).
57. White, D. A., Fink, D. & Gore, D. B. Cosmogenic nuclide evidence for enhanced sensitivity of an East Antarctic ice stream to change during the last deglaciation. *Geology* **39**, 23–26 (2011).
58. Mackintosh, A. *et al.* Exposure ages from mountain dipsticks in Mac. Robertson Land, East Antarctica, indicate little change in ice-sheet thickness since the Last Glacial Maximum. *Geology* **35**, 551–554 (2007).
59. Yamane, M. *et al.* The last deglacial history of Lützow-Holm Bay, East Antarctica. *J. Quat. Sci.* **26**, 3–6 (2011).
60. Spector, P., Stone, J. & Goehring, B. Thickness of the divide and flank of the West Antarctic Ice Sheet through the last deglaciation. *The Cryosphere* **13**, 3061–3075 (2019).
61. Bentley, M. J. *et al.* Deglacial history of the Pensacola Mountains, Antarctica from glacial geomorphology and cosmogenic nuclide surface exposure dating. *Quat. Sci. Rev.* **158**, 58–76 (2017).

62. Balco, G. *et al.* Cosmogenic-nuclide exposure ages from the Pensacola Mountains adjacent to the Foundation Ice Stream, Antarctica. *Am. J. Sci.* **316**, 542–577 (2016).
63. Hein, A. S. *et al.* Mid-Holocene pulse of thinning in the Weddell Sea sector of the West Antarctic ice sheet. *Nat. Commun.* **7**, (2016).
64. Bentley, M. J., Fogwill, C. J., Kubik, P. W. & Sugden, D. E. Geomorphological evidence and cosmogenic  $^{10}\text{Be}/^{26}\text{Al}$  exposure ages for the Last Glacial Maximum and deglaciation of the Antarctic Peninsula Ice Sheet. *Geol. Soc. Am. Bull.* **118**, 1149–1159 (2006).
65. Jeong, A. *et al.* Late Quaternary deglacial history across the Larsen B embayment, Antarctica. *Quat. Sci. Rev.* **189**, 134–148 (2018).
66. Glasser, N. F. *et al.* Ice-stream initiation, duration and thinning on James Ross Island, northern Antarctic Peninsula. *Quat. Sci. Rev.* **86**, 78–88 (2014).
67. Balco, G. & Schaefer, J. M. Exposure-age record of Holocene ice sheet and ice shelf change in the northeast Antarctic Peninsula. *Quat. Sci. Rev.* **59**, 101–111 (2013).
68. Johnson, J. S., Bentley, M. J., Roberts, S. J., Binnie, S. A. & Freeman, S. P. H. T. Holocene deglacial history of the northeast Antarctic Peninsula – A review and new chronological constraints. *Quat. Sci. Rev.* **30**, 3791–3802 (2011).
69. Bentley, M. J. *et al.* Rapid deglaciation of Marguerite Bay, western Antarctic Peninsula in the Early Holocene. *Quat. Sci. Rev.* **30**, 3338–3349 (2011).
70. Johnson, J. S., Nichols, K. A., Goehring, B. M., Balco, G. & Schaefer, J. M. Abrupt mid-Holocene ice loss in the western Weddell Sea Embayment of Antarctica. *Earth Planet. Sci. Lett.* **518**, 127–135 (2019).
71. Stenni, B. *et al.* The deuterium excess records of EPICA Dome C and Dronning Maud Land ice cores (East Antarctica). *Quat. Sci. Rev.* **29**, 146–159 (2010).
72. Parrenin, F. *et al.* 1-D-ice flow modelling at EPICA Dome C and Dome Fuji, East Antarctica. *Clim. Past* **3**, 243–259 (2007).
73. Delmotte, M., Raynaud, D., Morgan, V. & Jouzel, J. Climatic and glaciological information inferred from air-content measurements of a Law Dome (East Antarctica) ice core. *J. Glaciol.* **45**, 255–263 (1999).
74. Ommen, T. D. V., Morgan, V. & Curran, M. A. J. Deglacial and Holocene changes in accumulation at Law Dome, East Antarctica. *Ann. Glaciol.* **39**, 359–365 (2004).
75. Winski, D. A. *et al.* The SP19 chronology for the South Pole Ice Core – Part 1: volcanic matching and annual layer counting. *Clim. Past* **15**, 1793–1808 (2019).
76. Lilien, D. A. *et al.* Holocene Ice-Flow Speedup in the Vicinity of the South Pole. *Geophys. Res. Lett.* **45**, 6557–6565 (2018).
77. Fudge, T. J. *et al.* Variable relationship between accumulation and temperature in West Antarctica for the past 31,000 years. *Geophys. Res. Lett.* **43**, 3795–3803 (2016).
78. Koutnik, M. R. *et al.* Holocene accumulation and ice flow near the West Antarctic Ice Sheet Divide ice core site. *J. Geophys. Res. Earth Surf.* **121**, 907–924 (2016).
79. Stenni, B. *et al.* Expression of the bipolar see-saw in Antarctic climate records during the last deglaciation. *Nat. Geosci.* **4**, 46–49 (2011).
80. Hillenbrand, C.-D. *et al.* Grounding-line retreat of the West Antarctic Ice Sheet from inner Pine Island Bay. *Geology* **41**, 35–38 (2013).
81. Bart, P. J., DeCesare, M., Rosenheim, B. E., Majewski, W. & McGlannan, A. A centuries-long delay between a paleo-ice-shelf collapse and grounding-line retreat in the Whales Deep Basin, eastern Ross Sea, Antarctica. *Sci. Rep.* **8**, 12392 (2018).
82. McKay, R. *et al.* Antarctic marine ice-sheet retreat in the Ross Sea during the early Holocene. *Geology* **44**, 7–10 (2016).

83. Neuhaus, S. U. *et al.* Did Holocene climate changes drive West Antarctic grounding line retreat and re-advance? *The Cryosphere* **15**, 4655–4673 (2021).
84. Baroni, C. & Hall, B. L. A new Holocene relative sea-level curve for Terra Nova Bay, Victoria Land, Antarctica. *J. Quat. Sci.* **19**, 377–396 (2004).
85. Hemer, M. A. & Harris, P. T. Sediment core from beneath the Amery Ice Shelf, East Antarctica, suggests mid-Holocene ice-shelf retreat. *Geology* **31**, 127–130 (2003).
86. Hemer, M. A. *et al.* Sedimentological signatures of the sub-Amery Ice Shelf circulation. *Antarct. Sci.* **19**, 497–506 (2007).
87. Zwartz, D., Bird, M., Stone, J. & Lambeck, K. Holocene sea-level change and ice-sheet history in the Vestfold Hills, East Antarctica. *Earth Planet. Sci. Lett.* **155**, 131–145 (1998).
88. Verleyen, E., Hodgson, D. A., Milne, G. A., Sabbe, K. & Vyverman, W. Relative sea-level history from the Lambert Glacier region, East Antarctica, and its relation to deglaciation and Holocene glacier readvance. *Quat. Res.* **63**, 45–52 (2005).
89. Goodwin, I. D. & Zweck, C. Glacio-isostasy and Glacial Ice Load at Law Dome, Wilkes Land, East Antarctica. *Quat. Res.* **53**, 285–293 (2000).
90. Mackintosh, A. N. *et al.* Retreat history of the East Antarctic Ice Sheet since the Last Glacial Maximum. *Quat. Sci. Rev.* **100**, 10–30 (2014).
91. Miura H., Maemoku H., Seto K. & Moriwaki K. Late Quaternary East Antarctic melting event in the Soya Coast region based on stratigraphy and oxygen isotopic ratio of fossil molluscs. **11**, 260–274 (1998).
92. Arndt, J. E., Hillenbrand, C.-D., Grobe, H., Kuhn, G. & Wacker, L. Evidence for a dynamic grounding line in outer Filchner Trough, Antarctica, until the early Holocene. *Geology* **45**, 1035–1038 (2017).
93. Hodgson, D. A. *et al.* Deglaciation and future stability of the Coats Land ice margin, Antarctica. *The Cryosphere* **12**, 2383–2399 (2018).
94. Arndt, J. E. *et al.* Past ice sheet–seabed interactions in the northeastern Weddell Sea embayment, Antarctica. *The Cryosphere* **14**, 2115–2135 (2020).
95. Crawford, K., Kuhn, G. & Hambrey, M. J. Changes in the character of glaciomarine sedimentation in the southwestern Weddell Sea, Antarctica: evidence from the core PS1423-2. *Ann. Glaciol.* **22**, 200–204 (1996).
96. Hillenbrand, C.-D. *et al.* Reconstruction of changes in the Weddell Sea sector of the Antarctic Ice Sheet since the Last Glacial Maximum. *Quat. Sci. Rev.* **100**, 111–136 (2014).
97. Cofaigh, C. Ó. *et al.* Reconstruction of ice-sheet changes in the Antarctic Peninsula since the Last Glacial Maximum. *Quat. Sci. Rev.* **100**, 87–110 (2014).
98. Smith, J. A. *et al.* History of the Larsen C Ice Shelf reconstructed from sub–ice shelf and offshore sediments. *Geology* **49**, 978–982 (2021).
99. Peck, V. L., Allen, C. S., Kender, S., McClymont, E. L. & Hodgson, D. A. Oceanographic variability on the West Antarctic Peninsula during the Holocene and the influence of upper circumpolar deep water. *Quat. Sci. Rev.* **119**, 54–65 (2015).
100. Bentley, M. J., Hodgson, D. A., Smith, J. A. & Cox, N. J. Relative sea level curves for the South Shetland Islands and Marguerite Bay, Antarctic Peninsula. *Quat. Sci. Rev.* **24**, 1203–1216 (2005).
101. Watcham, E. P. *et al.* A new Holocene relative sea level curve for the South Shetland Islands, Antarctica. *Quat. Sci. Rev.* **30**, 3152–3170 (2011).

102. Pollard, D., Gomez, N., DeConto, R. & Han, H. Estimating Modern Elevations of Pliocene Shorelines Using a Coupled Ice Sheet-Earth-Sea Level Model. *J. Geophys. Res. Earth Surf.* **123**, 2279–2291 (2018).
103. Tigchelaar, M., Timmermann, A., Pollard, D., Friedrich, T. & Heinemann, M. Local insolation changes enhance Antarctic interglacials: Insights from an 800,000-year ice sheet simulation with transient climate forcing. *Earth Planet. Sci. Lett.* **495**, 69–78 (2018).
104. Lowry, D. P., Golledge, N. R., Bertler, N. A., Jones, R. S. & McKay, R. Deglacial grounding-line retreat in the Ross Embayment, Antarctica, controlled by ocean and atmosphere forcing. *Sci. Adv.* **5**, eaav8754 (2019).
105. Johnson, J. S. *et al.* Comparing Glacial-Geological Evidence and Model Simulations of Ice Sheet Change since the Last Glacial Period in the Amundsen Sea Sector of Antarctica. *J. Geophys. Res. Earth Surf.* **126**, e2020JF005827 (2021).
106. Lowry, D. P. *et al.* Geologic controls on ice sheet sensitivity to deglacial climate forcing in the Ross Embayment, Antarctica. *Quat. Sci. Adv.* **1**, 100002 (2020).
107. Albrecht, T., Winkelmann, R. & Levermann, A. Glacial-cycle simulations of the Antarctic Ice Sheet with the Parallel Ice Sheet Model (PISM) – Part 1: Boundary conditions and climatic forcing. *The Cryosphere* **14**, 599–632 (2020).
108. Jones, R., Whitehouse, P., Bentley, M., Small, D. & Dalton, A. Impact of glacial isostatic adjustment on cosmogenic surface-exposure dating. *Quat. Sci. Rev.* **212**, 206–212 (2019).
109. Hillenbrand, C.-D. *et al.* West Antarctic Ice Sheet retreat driven by Holocene warm water incursions. *Nature* **547**, 43–48 (2017).
110. Shevenell, A. E., Ingalls, A. E., Domack, E. W. & Kelly, C. Holocene Southern Ocean surface temperature variability west of the Antarctic Peninsula. *Nature* **470**, 250–4 (2011).
111. Etourneau, J. *et al.* Ocean temperature impact on ice shelf extent in the eastern Antarctic Peninsula. *Nat. Commun.* **10**, 304 (2019).
112. Kim, J. *et al.* Holocene subsurface temperature variability in the eastern Antarctic continental margin. *Geophys. Res. Lett.* **39**, L06705 (2012).
113. Jones, R. S., Gudmundsson, G. H., Mackintosh, A., McCormack, F. & Whitmore, R. J. Ocean-driven and topography-controlled nonlinear glacier retreat during the Holocene: southwestern Ross Sea, Antarctica. *Geophys. Res. Lett.* (2021) doi:10.1029/2020GL091454.
114. Whitehouse, P. L. *et al.* Controls on last glacial maximum ice extent in the Weddell Sea embayment, Antarctica. *J. Geophys. Res. Earth Surf.* **122**, 371–397 (2017).
115. Jamieson, S. S. *et al.* Ice-stream stability on a reverse bed slope. *Nat. Geosci.* **5**, 799–802 (2012).
116. Johnson, J. S. *et al.* Review article: Existing and potential evidence for Holocene grounding-line retreat and readvance in Antarctica. *The Cryosphere* **16**, 1543–1562 (2022).
117. Siegert, M., Ross, N., Corr, H., Kingslake, J. & Hindmarsh, R. Late Holocene ice-flow reconfiguration in the Weddell Sea sector of West Antarctica. *Quat. Sci. Rev.* **78**, 98–107 (2013).
118. Bingham, R. G. *et al.* Ice-flow structure and ice dynamic changes in the Weddell Sea sector of West Antarctica from radar-imaged internal layering. *J. Geophys. Res. Earth Surf.* **120**, 655–670 (2015).

119. Winter, K. *et al.* Airborne radar evidence for tributary flow switching in Institute Ice Stream, West Antarctica: Implications for ice sheet configuration and dynamics. *J. Geophys. Res. Earth Surf.* **120**, 1611–1625 (2015).
120. Kingslake, J., Martín, C., Arthern, R. J., Corr, H. F. J. & King, E. C. Ice-flow reorganization in West Antarctica 2.5 kyr ago dated using radar-derived englacial flow velocities. *Geophys. Res. Lett.* **43**, 9103–9112 (2016).
121. Bradley, S. L., Hindmarsh, R. C., Whitehouse, P. L., Bentley, M. J. & King, M. A. Low post-glacial rebound rates in the Weddell Sea due to Late Holocene ice-sheet readvance. *Earth Planet. Sci. Lett.* **413**, 79–89 (2015).
122. Wearing, M. G. & Kingslake, J. Holocene Formation of Henry Ice Rise, West Antarctica, Inferred From Ice-Penetrating Radar. *J. Geophys. Res. Earth Surf.* **124**, 2224–2240 (2019).
123. Ashmore, D. W. *et al.* Englacial Architecture and Age-Depth Constraints Across the West Antarctic Ice Sheet. *Geophys. Res. Lett.* **47**, e2019GL086663 (2020).
124. Bentley, M. J. *et al.* Early Holocene retreat of the George VI Ice Shelf, Antarctic Peninsula. *Geology* **33**, 173 (2005).
125. Domack, E. W., Jull, A. T. & Nakao, S. Advance of East Antarctic outlet glaciers during the Hypsithermal: implications for the volume state of the Antarctic ice sheet under global warming. *Geology* **19**, 1059–1062 (1991).
126. Goodwin, I. D. A mid to late Holocene readvance of the Law Dome ice margin, Budd Coast, East Antarctica. *Antarct. Sci.* **8**, 395–406 (1996).
127. Hall. Holocene glacial history of Antarctica and the sub-Antarctic islands. *Quat. Sci. Rev.* **28**, 2213–2230 (2009).
128. Kaplan, M. R. *et al.* Holocene glacier behavior around the northern Antarctic Peninsula and possible causes. *Earth Planet. Sci. Lett.* **534**, 116077 (2020).
129. Simms, A. R. *et al.* Evidence for a “Little Ice Age” glacial advance within the Antarctic Peninsula – Examples from glacially-overrun raised beaches. *Quat. Sci. Rev.* **271**, 107195 (2021).
130. King, M. A., Watson, C. S. & White, D. GPS Rates of Vertical Bedrock Motion Suggest Late Holocene Ice-Sheet Readvance in a Critical Sector of East Antarctica. *Geophys. Res. Lett.* **49**, e2021GL097232 (2022).
131. Larour, E. *et al.* Slowdown in Antarctic mass loss from solid Earth and sea-level feedbacks. *Science* **364**, eaav7908 (2019).
132. Das, S. B. & Alley, R. B. Rise in frequency of surface melting at Siple Dome through the Holocene: Evidence for increasing marine influence on the climate of West Antarctica. *J. Geophys. Res. Atmospheres* **113**, (2008).
133. Hillebrand, T. R. *et al.* Holocene thinning of Darwin and Hatherton glaciers, Antarctica, and implications for grounding-line retreat in the Ross Sea. *The Cryosphere* **15**, 3329–3354 (2021).
134. Crespin, J. *et al.* Holocene glacial discharge fluctuations and recent instability in East Antarctica. *Earth Planet. Sci. Lett.* **394**, 38–47 (2014).
135. Crosta, X. *et al.* Ocean as the main driver of Antarctic ice sheet retreat during the Holocene. *Glob. Planet. Change* **166**, 62–74 (2018).
136. Bakker, P., Clark, P. U., Golledge, N. R., Schmittner, A. & Weber, M. E. Centennial-scale Holocene climate variations amplified by Antarctic Ice Sheet discharge. *Nature* **541**, 72–76 (2017).

137. Dickens, W. A. *et al.* Enhanced glacial discharge from the eastern Antarctic Peninsula since the 1700s associated with a positive Southern Annular Mode. *Sci. Rep.* **9**, 14606 (2019).
138. Christ, A. J. *et al.* Late Holocene glacial advance and ice shelf growth in Barilari Bay, Graham Land, west Antarctic Peninsula. *Geol. Soc. Am. Bull.* **127**, 297–315 (2015).
139. Domack, E. W. & McClennen, C. E. Accumulation of glacial marine sediments in fjords of the Antarctic Peninsula and their use as late Holocene paleoenvironmental indicators. *Found. Ecol. Res. West Antarct. Penins.* **70**, 135–154 (1996).
140. Simms, A. R. *et al.* Late Holocene relative sea levels near Palmer Station, northern Antarctic Peninsula, strongly controlled by late Holocene ice-mass changes. *Quat. Sci. Rev.* **199**, 49–59 (2018).
141. Zurbuchen, J. & Simms, A. R. Late Holocene ice-mass changes recorded in a relative sea-level record from Joinville Island, Antarctica. *Geology* **47**, 1064–1068 (2019).
142. Ashley, K. E. *et al.* Mid-Holocene Antarctic sea-ice increase driven by marine ice sheet retreat. *Clim. Past* **17**, 1–19 (2021).
143. Minzoni, R. T. *et al.* Oceanographic influences on the stability of the Cosgrove Ice Shelf, Antarctica. *The Holocene* **27**, 1645–1658 (2017).
144. Abram, N. J. *et al.* Evolution of the Southern Annular Mode during the past millennium. *Nat. Clim. Change* **4**, 564–569 (2014).
145. Mulvaney, R. *et al.* Recent Antarctic Peninsula warming relative to Holocene climate and ice-shelf history. *Nature* **489**, 141–144 (2012).
146. Frezzotti, M., Scarchilli, C., Becagli, S., Proposito, M. & Urbini, S. A synthesis of the Antarctic surface mass balance during the last 800 yr. *The Cryosphere* **7**, 303–319 (2013).
147. Bertler, N. A. N., Mayewski, P. A. & Carter, L. Cold conditions in Antarctica during the Little Ice Age — Implications for abrupt climate change mechanisms. *Earth Planet. Sci. Lett.* **308**, 41–51 (2011).
148. Medley, B. & Thomas, E. R. Increased snowfall over the Antarctic Ice Sheet mitigated twentieth-century sea-level rise. *Nat. Clim. Change* **9**, 34–39 (2019).
149. Jones, J. M. *et al.* Assessing recent trends in high-latitude Southern Hemisphere surface climate. *Nat. Clim. Change* **6**, 917–926 (2016).
150. Jones, R. *et al.* Cosmogenic nuclides constrain surface fluctuations of an East Antarctic outlet glacier since the Pliocene. *Earth Planet. Sci. Lett.* **480**, 75–86 (2017).
151. Bockheim, J. G., Wilson, S. C., Denton, G. H., Andersen, B. G. & Stuiver, M. Late Quaternary ice-surface fluctuations of Hatherton Glacier, Transantarctic Mountains. *Quat. Res.* **31**, 229–254 (1989).
152. Bentley, M. J. *et al.* Deglacial history of the West Antarctic Ice Sheet in the Weddell Sea embayment: Constraints on past ice volume change. *Geology* **38**, 411–414 (2010).
153. Todd, C., Stone, J., Conway, H., Hall, B. & Bromley, G. Late Quaternary evolution of Reedy Glacier, Antarctica. *Quat. Sci. Rev.* **29**, 1328–1341 (2010).
154. Brachfeld, S. *et al.* Holocene history of the Larsen-A Ice Shelf constrained by geomagnetic paleointensity dating. *Geology* **31**, 749–752 (2003).
155. Hulbe, C. & Fahnestock, M. Century-scale discharge stagnation and reactivation of the Ross ice streams, West Antarctica. *J. Geophys. Res.* **112**, (2007).
156. Smith, J. A. *et al.* Sub-ice-shelf sediments record history of twentieth-century retreat of Pine Island Glacier. *Nature* **541**, 77–80 (2017).
157. Ullman, D. J. *et al.* Final Laurentide ice-sheet deglaciation and Holocene climate-sea level change. *Quat. Sci. Rev.* **152**, 49–59 (2016).



158. Larsen, N. K. *et al.* The response of the southern Greenland ice sheet to the Holocene thermal maximum. *Geology* **43**, 291–294 (2015).
159. Briner, J. P. *et al.* Rate of mass loss from the Greenland Ice Sheet will exceed Holocene values this century. *Nature* **586**, 70–74 (2020).
160. Hughes, A. L., Gyllencreutz, R., Lohne, Ø. S., Mangerud, J. & Svendsen, J. I. The last Eurasian ice sheets—a chronological database and time-slice reconstruction, DATED-1. *Boreas* **45**, 1–45 (2016).
161. Cuzzone, J. K. *et al.* Final deglaciation of the Scandinavian Ice Sheet and implications for the Holocene global sea-level budget. *Earth Planet. Sci. Lett.* **448**, 34–41 (2016).
162. Simms, A. R., Lisiecki, L., Gebbie, G., Whitehouse, P. L. & Clark, J. F. Balancing the last glacial maximum (LGM) sea-level budget. *Quat. Sci. Rev.* **205**, 143–153 (2019).
163. Gowan, E. J. *et al.* A new global ice sheet reconstruction for the past 80 000 years. *Nat. Commun.* **12**, 1199 (2021).
164. Chua, S. *et al.* A new Holocene sea-level record for Singapore. *The Holocene* **31**, 1376–1390 (2021).
165. Engelhart, S. E. & Horton, B. P. Holocene sea level database for the Atlantic coast of the United States. *Quat. Sci. Rev.* **54**, 12–25 (2012).
166. Khan, N. S. *et al.* Drivers of Holocene sea-level change in the Caribbean. *Quat. Sci. Rev.* **155**, 13–36 (2017).
167. Hijma, M. P. & Cohen, K. M. Holocene sea-level database for the Rhine-Meuse Delta, The Netherlands: Implications for the pre-8.2 ka sea-level jump. *Quat. Sci. Rev.* **214**, 68–86 (2019).
168. García-Artola, A. *et al.* Holocene sea-level database from the Atlantic coast of Europe. *Quat. Sci. Rev.* **196**, 177–192 (2018).
169. Cooper, J. A. G., Green, A. N. & Compton, J. S. Sea-level change in southern Africa since the Last Glacial Maximum. *Quat. Sci. Rev.* **201**, 303–318 (2018).
170. Bard, E., Hamelin, B. & Delanghe-Sabatier, D. Deglacial meltwater pulse 1B and Younger Dryas sea levels revisited with boreholes at Tahiti. *Science* **327**, 1235–7 (2010).
171. Nakada, M. & Lambeck, K. Late Pleistocene and Holocene sea-level change in the Australian region and mantle rheology. *Geophys. J. Int.* **96**, 497–517 (1989).
172. Clement, A. J. H., Whitehouse, P. L. & Sloss, C. R. An examination of spatial variability in the timing and magnitude of Holocene relative sea-level changes in the New Zealand archipelago. *Quat. Sci. Rev.* **131**, 73–101 (2016).
173. Mauz, B., Ruggieri, G. & Spada, G. Terminal Antarctic melting inferred from a far-field coastal site. *Quat. Sci. Rev.* **116**, 122–132 (2015).
174. Milne, G., Long, A. & Bassett, S. Modelling Holocene relative sea-level observations from the Caribbean and South America. *Quat. Sci. Rev.* **24**, 1183–1202 (2005).
175. Horton, B. P. *et al.* Holocene sea levels and palaeoenvironments, Malay-Thai Peninsula, southeast Asia. *The Holocene* **15**, 1199–1213 (2005).
176. Nunn, P. D. & Peltier, W. R. Far-Field Test of the ICE-4G Model of Global Isostatic Response to Deglaciation Using Empirical and Theoretical Holocene Sea-Level Reconstructions for the Fiji Islands, Southwestern Pacific. *Quat. Res.* **55**, 203–214 (2001).
177. Peltier, W. R. On eustatic sea level history: Last Glacial Maximum to Holocene. *Quat. Sci. Rev.* **21**, 377–396 (2002).

178. Roy, K. & Peltier, W. R. Relative sea level in the Western Mediterranean basin: A regional test of the ICE-7G\_NA (VM7) model and a constraint on late Holocene Antarctic deglaciation. *Quat. Sci. Rev.* **183**, 76–87 (2018).
179. Yokoyama, Y. *et al.* Holocene sea-level change and Antarctic melting history derived from geological observations and geophysical modeling along the Shimokita Peninsula, northern Japan. *Geophys. Res. Lett.* **39**, n/a-n/a (2012).
180. Yokoyama, Y. *et al.* Holocene Indian Ocean sea level, Antarctic melting history and past Tsunami deposits inferred using sea level reconstructions from the Sri Lankan, Southeastern Indian and Maldivian coasts. *Quat. Sci. Rev.* **206**, 150–161 (2019).
181. Bradley, S. L., Milne, G. A., Horton, B. P. & Zong, Y. Modelling sea level data from China and Malay-Thailand to estimate Holocene ice-volume equivalent sea level change. *Quat. Sci. Rev.* **137**, 54–68 (2016).
182. Tam, C.-Y. *et al.* A below-the-present late Holocene relative sea level and the glacial isostatic adjustment during the Holocene in the Malay Peninsula. *Quat. Sci. Rev.* **201**, 206–222 (2018).
183. Kemp, A. C. *et al.* Relative sea-level change in Newfoundland, Canada during the past ~3000 years. *Quat. Sci. Rev.* **201**, 89–110 (2018).
184. Törnqvist, T. E., Jankowski, K. L., Li, Y.-X. & González, J. L. Tipping points of Mississippi Delta marshes due to accelerated sea-level rise. *Sci. Adv.* **6**, eaaz5512 (2020).
185. Shennan, I., Bradley, S. L. & Edwards, R. Relative sea-level changes and crustal movements in Britain and Ireland since the Last Glacial Maximum. *Quat. Sci. Rev.* **188**, 143–159 (2018).
186. Vacchi, M. *et al.* Multiproxy assessment of Holocene relative sea-level changes in the western Mediterranean: Sea-level variability and improvements in the definition of the isostatic signal. *Earth-Sci. Rev.* **155**, 172–197 (2016).
187. Hallmann, N. *et al.* Ice volume and climate changes from a 6000 year sea-level record in French Polynesia. *Nat. Commun.* **9**, 285 (2018).
188. Woodroffe, S. A., Long, A. J., Milne, G. A., Bryant, C. L. & Thomas, A. L. New constraints on late Holocene eustatic sea-level changes from Mahé, Seychelles. *Quat. Sci. Rev.* **115**, 1–16 (2015).
189. Sloss, C. R., Murray-Wallace, C. V. & Jones, B. G. Holocene sea-level change on the southeast coast of Australia: a review. *The Holocene* **17**, 999–1014 (2007).
190. Mann, T. *et al.* Holocene sea levels in Southeast Asia, Maldives, India and Sri Lanka: The SEAMIS database. *Quat. Sci. Rev.* **219**, 112–125 (2019).
191. Mitrovica, J. X. & Milne, G. A. On the origin of late Holocene sea-level highstands within equatorial ocean basins. *Quat. Sci. Rev.* **21**, 2179–2190 (2002).
192. Meltzner, A. J. *et al.* Half-metre sea-level fluctuations on centennial timescales from mid-Holocene corals of Southeast Asia. *Nat. Commun.* **8**, 14387 (2017).
193. Fox-Kemper, B. *et al.* Ocean, cryosphere, and sea level change. in *Climate Change 2021: The Physical Science Basis. Contribution of Working Group I to the Sixth Assessment Report of the Intergovernmental Panel on Climate Change* (eds. Masson-Delmotte, V. *et al.*) (Cambridge University Press, 2021).
194. Church, J. A., Gregory, J. M., White, N. J., Platten, S. M. & Mitrovica, J. X. Understanding and Projecting Sea Level Change. *Oceanography* **24**, 130–143 (2011).
195. Walker, J. S., Kopp, R. E., Little, C. M. & Horton, B. P. Timing of emergence of modern rates of sea-level rise by 1863. *Nat. Commun.* **13**, 966 (2022).

196. Schmidtko, S., Heywood, K. J., Thompson, A. F. & Aoki, S. Multidecadal warming of Antarctic waters. *Science* **346**, 1227–1231 (2014).
197. Joughin, I., Smith, B. E. & Medley, B. Marine Ice Sheet Collapse Potentially Under Way for the Thwaites Glacier Basin, West Antarctica. *Science* **344**, 735–738 (2014).
198. Favier, L. *et al.* Retreat of Pine Island Glacier controlled by marine ice-sheet instability. *Nat. Clim. Change* **2**, 117 (2014).
199. Robel, A. A., Seroussi, H. & Roe, G. H. Marine ice sheet instability amplifies and skews uncertainty in projections of future sea-level rise. *Proc. Natl. Acad. Sci.* **116**, 14887–14892 (2019).
200. Scambos, T. A., Bohlander, J., Shuman, C. u & Skvarca, P. Glacier acceleration and thinning after ice shelf collapse in the Larsen B embayment, Antarctica. *Geophys. Res. Lett.* **31**, (2004).
201. Hogg, A. E. & Gudmundsson, G. H. Impacts of the Larsen-C Ice Shelf calving event. *Nat. Clim. Change* **7**, 540–542 (2017).
202. Domack, E. *et al.* Stability of the Larsen B ice shelf on the Antarctic Peninsula during the Holocene epoch. *Nature* **436**, 681–685 (2005).
203. Seroussi, H. *et al.* ISMIP6 Antarctica: a multi-model ensemble of the Antarctic ice sheet evolution over the 21st century. *The Cryosphere* **14**, 3033–3070 (2020).
204. Sutter, J., Fischer, H. & Eisen, O. Investigating the internal structure of the Antarctic ice sheet: the utility of isochrones for spatiotemporal ice-sheet model calibration. *The Cryosphere* **15**, 3839–3860 (2021).
205. Spector, P. *et al.* West Antarctic sites for subglacial drilling to test for past ice-sheet collapse. *The Cryosphere* **12**, 2741–2757 (2018).
206. Stone, J. O. Air pressure and cosmogenic isotope production. *J. Geophys. Res. Solid Earth 1978–2012* **105**, 23753–23759 (2000).
207. Rosenheim, B. E., Santoro, J. A., Gunter, M. & Domack, E. W. Improving Antarctic Sediment 14C Dating Using Ramped Pyrolysis: An Example from the Hugo Island Trough. *Radiocarbon* **55**, 115–126 (2013).
208. Hall, B. L., Henderson, G. M., Baroni, C. & Kellogg, T. B. Constant Holocene Southern-Ocean 14C reservoir ages and ice-shelf flow rates. *Earth Planet. Sci. Lett.* **296**, 115–123 (2010).
209. Subt, C., Fangman, K. A., Wellner, J. S. & Rosenheim, B. E. Sediment chronology in Antarctic deglacial sediments: Reconciling organic carbon 14C ages to carbonate 14C ages using Ramped PyrOx. *The Holocene* **26**, 265–273 (2016).
210. Lifton, N. A., Jull, A. J. T. & Quade, J. A new extraction technique and production rate estimate for in situ cosmogenic 14C in quartz. *Geochim. Cosmochim. Acta* **65**, 1953–1969 (2001).
211. Nichols, K. A. *et al.* New Last Glacial Maximum ice thickness constraints for the Weddell Sea Embayment, Antarctica. *The Cryosphere* **13**, 2935–2951 (2019).
212. Pattyn, F., Favier, L., Sun, S. & Durand, G. Progress in Numerical Modeling of Antarctic Ice-Sheet Dynamics. *Curr. Clim. Change Rep.* **3**, 174–184 (2017).
213. Yokoyama, Y. & Purcell, A. On the geophysical processes impacting palaeo-sea-level observations. *Geosci. Lett.* **8**, 13 (2021).
214. Powell, E., Gomez, N., Hay, C., Latychev, K. & Mitrovica, J. X. Viscous Effects in the Solid Earth Response to Modern Antarctic Ice Mass Flux: Implications for Geodetic Studies of WAIS Stability in a Warming World. *J. Clim.* **33**, 443–459 (2020).

215. Bracegirdle, T. J. *et al.* Back to the Future: Using Long-Term Observational and Paleo-Proxy Reconstructions to Improve Model Projections of Antarctic Climate. *Geosciences* **9**, 255 (2019).
216. Nield, G. A. *et al.* Rapid bedrock uplift in the Antarctic Peninsula explained by viscoelastic response to recent ice unloading. *Earth Planet. Sci. Lett.* **397**, 32–41 (2014).
217. Lloyd, A. J. *et al.* Seismic structure of the Antarctic upper mantle imaged with adjoint tomography. *J. Geophys. Res. Solid Earth* **125**, (2020).
218. Balco, G. Technical note: A prototype transparent-middle-layer data management and analysis infrastructure for cosmogenic-nuclide exposure dating. *Geochronology* **2**, 169–175 (2020).
219. Larter, R. D. *et al.* Reconstruction of changes in the Amundsen Sea and Bellingshausen Sea sector of the West Antarctic Ice Sheet since the Last Glacial Maximum. *Quat. Sci. Rev.* **100**, 55–86 (2014).
220. Anderson, J. B. *et al.* Ross Sea paleo-ice sheet drainage and deglacial history during and since the LGM. *Quat. Sci. Rev.* **100**, 31–54 (2014).
221. Subt, C. *et al.* Sub-ice shelf sediment geochronology utilizing novel radiocarbon methodology for highly detrital sediments. *Geochem. Geophys. Geosystems* **18**, 1404–1418 (2017).
222. Minzoni, R. T., Anderson, J. B., Fernandez, R. & Wellner, J. S. Marine record of Holocene climate, ocean, and cryosphere interactions: Herbert Sound, James Ross Island, Antarctica. *Quat. Sci. Rev.* **129**, 239–259 (2015).
223. Berg, S., Melles, M., Gore, D. B., Verkulich, S. & Pushina, Z. V. Postglacial evolution of marine and lacustrine water bodies in Bunge Hills. *Antarct. Sci.* **32**, 107–129 (2020).
224. Braddock, S. *et al.* Relative sea-level data preclude major late Holocene ice-mass change in Pine Island Bay. *Nat. Geosci.* (2022).
225. Balco, G. Glacier Change and Paleoclimate Applications of Cosmogenic-Nuclide Exposure Dating. *Annu. Rev. Earth Planet. Sci.* **48**, 21–48 (2020).
226. Helsen, M. M. *et al.* Elevation Changes in Antarctica Mainly Determined by Accumulation Variability. *Science* **320**, 1626–1629 (2008).
227. Werner, M., Jouzel, J., Masson-Delmotte, V. & Lohmann, G. Reconciling glacial Antarctic water stable isotopes with ice sheet topography and the isotopic paleothermometer. *Nat. Commun.* **9**, 3537 (2018).
228. Simkins, L. M., Greenwood, S. L. & Anderson, J. B. Diagnosing ice sheet grounding line stability from landform morphology. *The Cryosphere* **12**, 2707–2726 (2018).
229. Roberts, S. J. *et al.* Holocene relative sea-level change and deglaciation on Alexander Island, Antarctic Peninsula, from elevated lake deltas. *Geomorphology* **112**, 122–134 (2009).

## **Acknowledgements**

R.S.J. is supported by the Australian Research Council (ARC) under grant number DE210101923. J.S.J. is supported by Natural Environment Research Council (NERC) grants NE/K012088/1 and NE/S006710/1. Y.L. is supported by China Scholarship Council–Durham University joint scholarship. J.A.S. is supported by NERC grant NE/M013081/1. This work was supported by ARC SRIEAS Grant SR200100005 Securing Antarctica’s Environmental Future, Australia, and forms part of the British Antarctic Survey programme “Polar Science for Planet Earth” funded by NERC, U.K.

## **Author contributions**

R.S.J. conceptualised the article, drafted the manuscript, and produced the figures. J.S.J., Y.L., A.N.M., J.P.S., J.A.S., E.R.T. and P.L.W. contributed to the assessment of literature, interpretation of data and discussion of section content, and Y.L. carried out the sea level modelling for Figure 6. All authors reviewed the manuscript prior to submission.

## **Competing interests**

The authors declare no competing interests.

## **Publisher's note**

Springer Nature remains neutral with regard to jurisdictional claims in published maps and institutional affiliations.